

Present Detection Methods



The Pierre Auger Observatory

Hybrid detection of extensive air showers

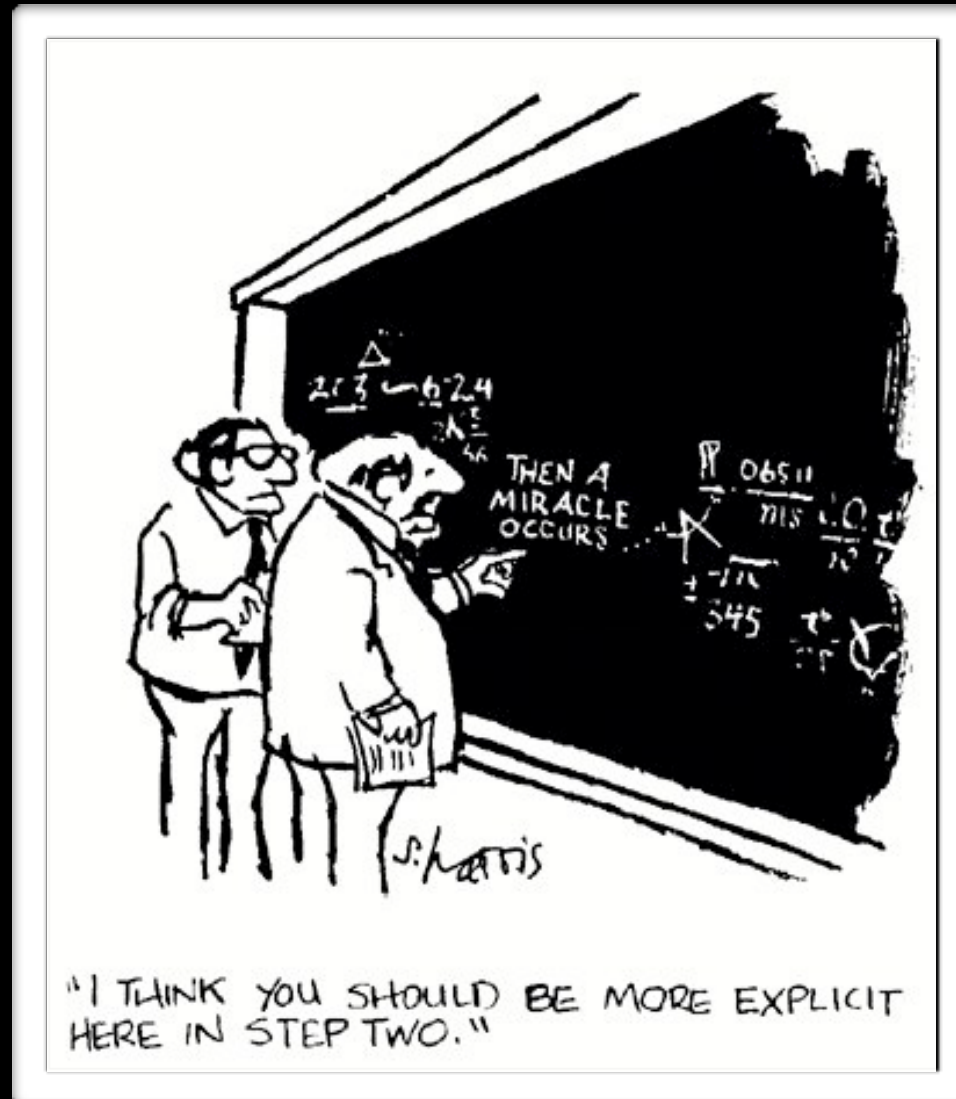
Water Cherenkov detectors

- lateral distributions on ground level
- ~100% duty cycle

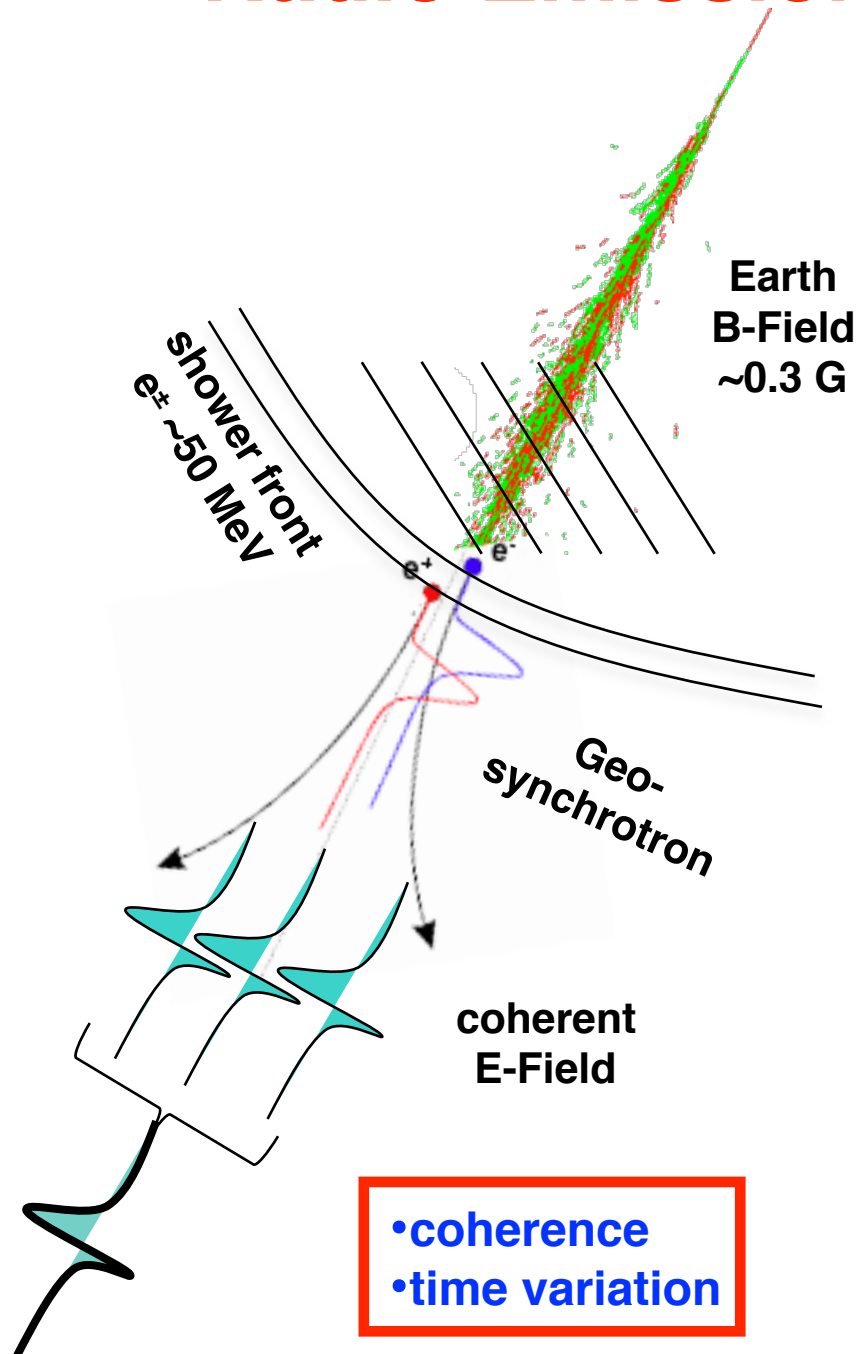
Fluorescence telescopes

- longitudinal shower development
- ~15 % duty cycle (moonless nights)
- light absorption by aerosols

Radio Emission



Radio Emission in Air Showers



- UHECRs produce particle showers in atmosphere
- Shower front is $\sim 2-3$ m thick
 \sim wavelength at 100 MHz
- e^\pm emit (mostly) synchrotron rad. in geomagnetic field
- Emissions from all e^\pm (N_e) add up coherently
- Radio power grows quadratically with N_e
- Mainly: Charge separation in geomagnetic field

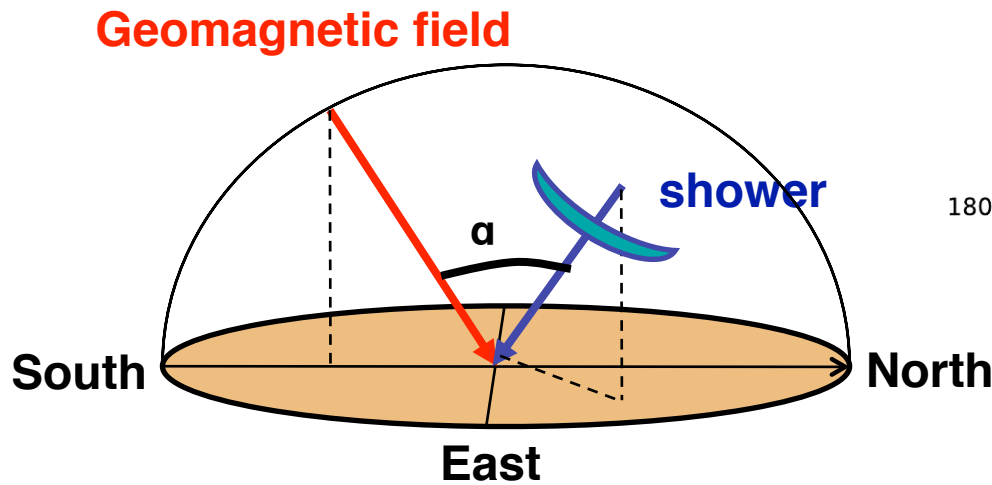
$$\vec{E} \propto \vec{v} \times \vec{B}$$

Theory predicts additional mechanisms:

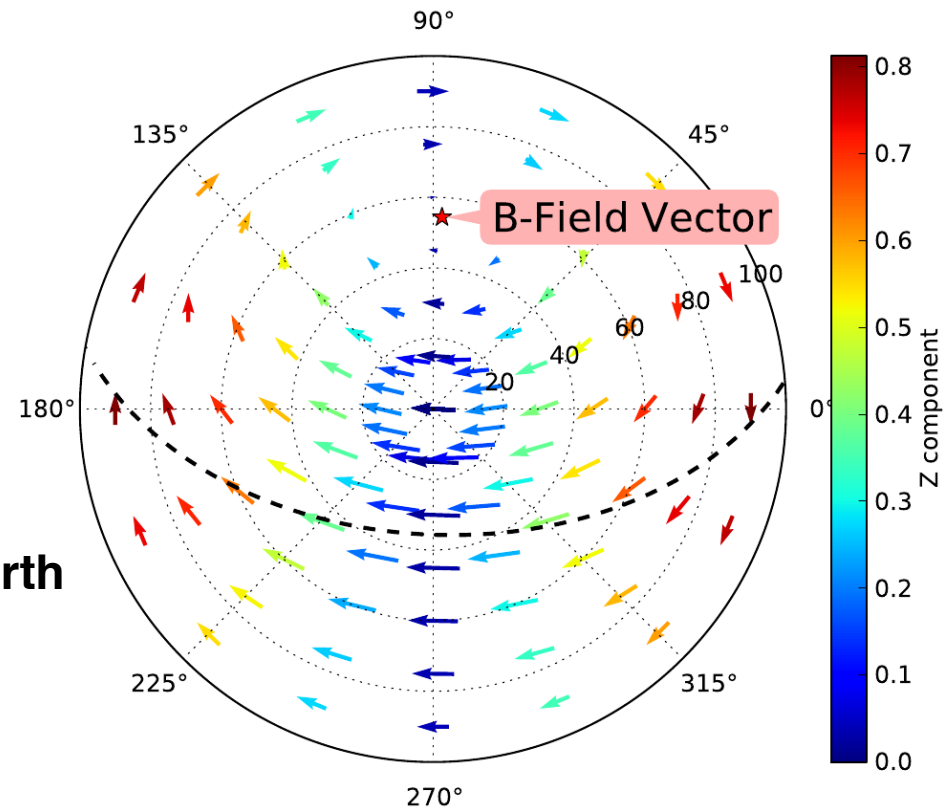
- excess of electrons in shower: charge excess
- superposition of emission due to Cherenkov effect in atmosphere

Synchrotron radiation in Geomagnetic Field

- radio emission dominated by geosynchrotron emission
- emission strength depends on angle to Earth's B field



$$\vec{\epsilon} \propto \vec{v} \times \vec{B}$$



expected polarisation
here simply $\mathbf{v} \times \mathbf{B}$

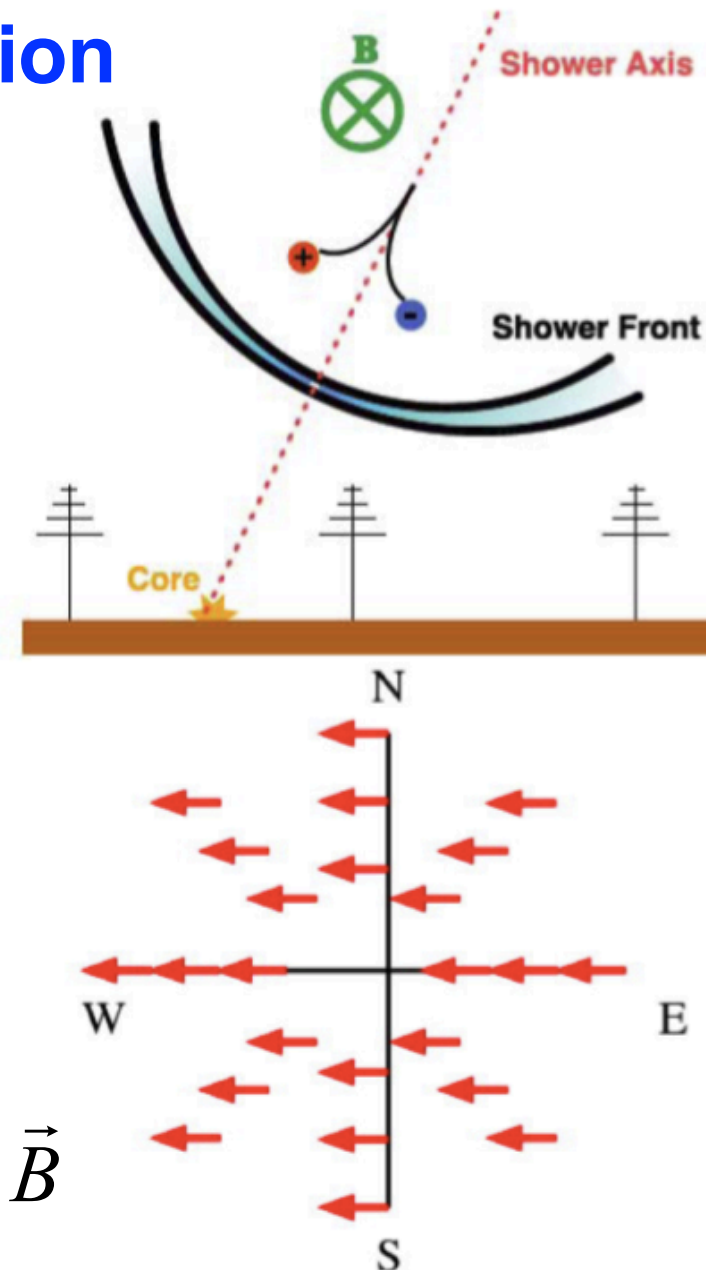
Radio Emission in Air Showers

1st order: geomagnetic emission

- *time-varying* transverse currents
- signal strength
 $\sim v \times B = v B \sin(\alpha)$
- purely linear polarisation
 - E-field vector aligned with $v \times B$ for all observer locations
- emission can be „compressed“ by Cherenkov effects

$$\vec{A} \propto \vec{J}_{Lorentz} \quad \vec{E} = \frac{d\vec{A}}{dt} \propto \vec{v} \times \vec{B}$$

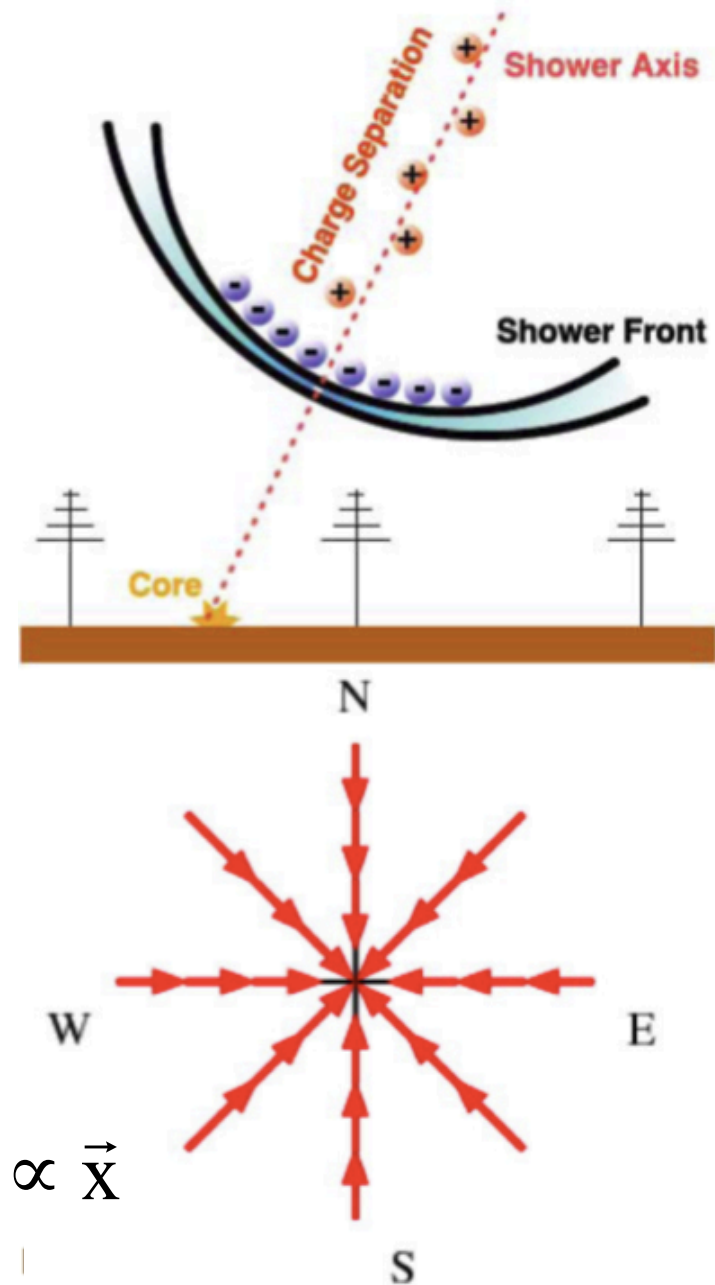
T. Huege, K. de Vries



Radio Emission in Air Showers

2nd order: Askaryan emission

- Askaryan: *time-varying* charge-excess
- also occurs for $n=1$!
- Cherenkov effects „compress“ the emission
- not „classical“ Cherenkov emission of a non-varying net charge
- linearly polarized
- E-field vector radially oriented, varies with observer location relative to core

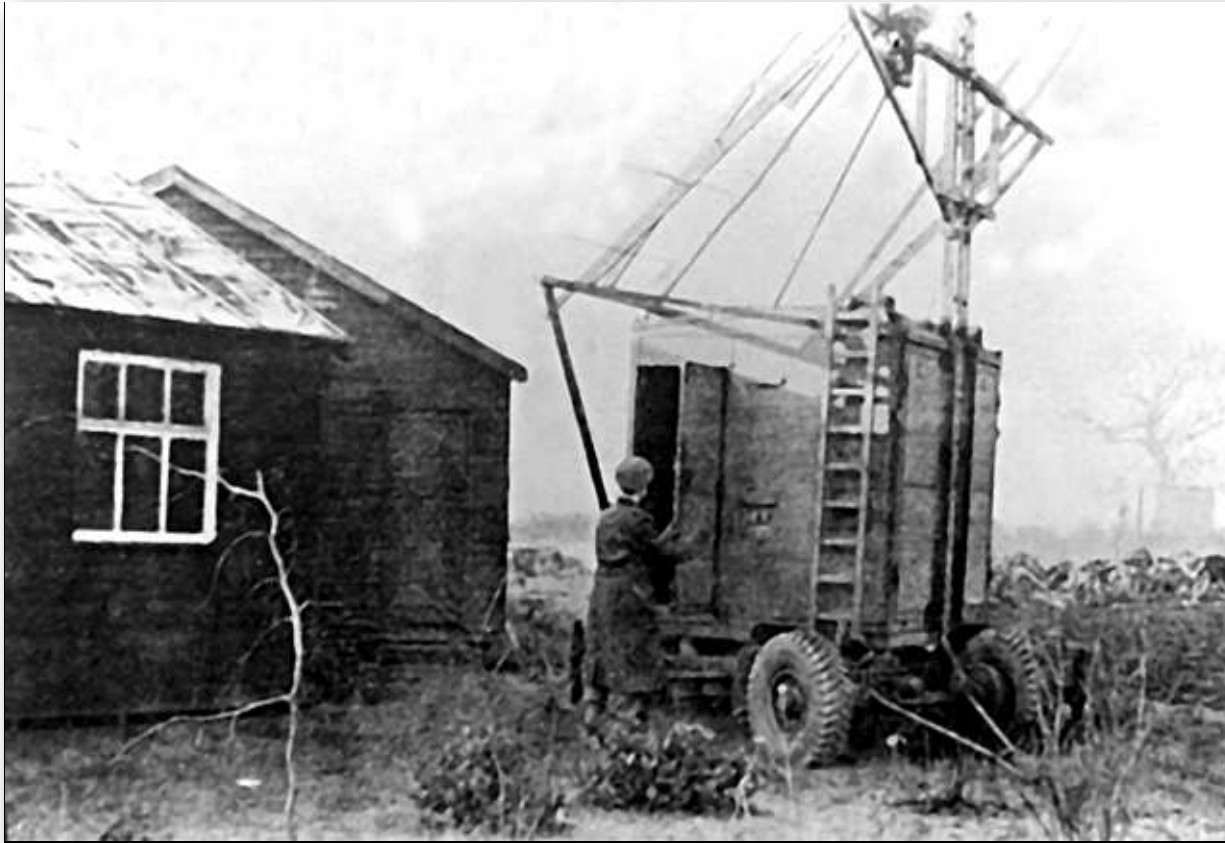


$$A \propto J^0 \quad \vec{E} = \frac{dA^0}{d\vec{x}} \propto \vec{x}$$

History



Jodrell Bank 1946

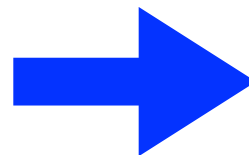


No air showers detected



No luck due to rapid attachment time (ns) of free electrons in the lower atmosphere (damping factor)

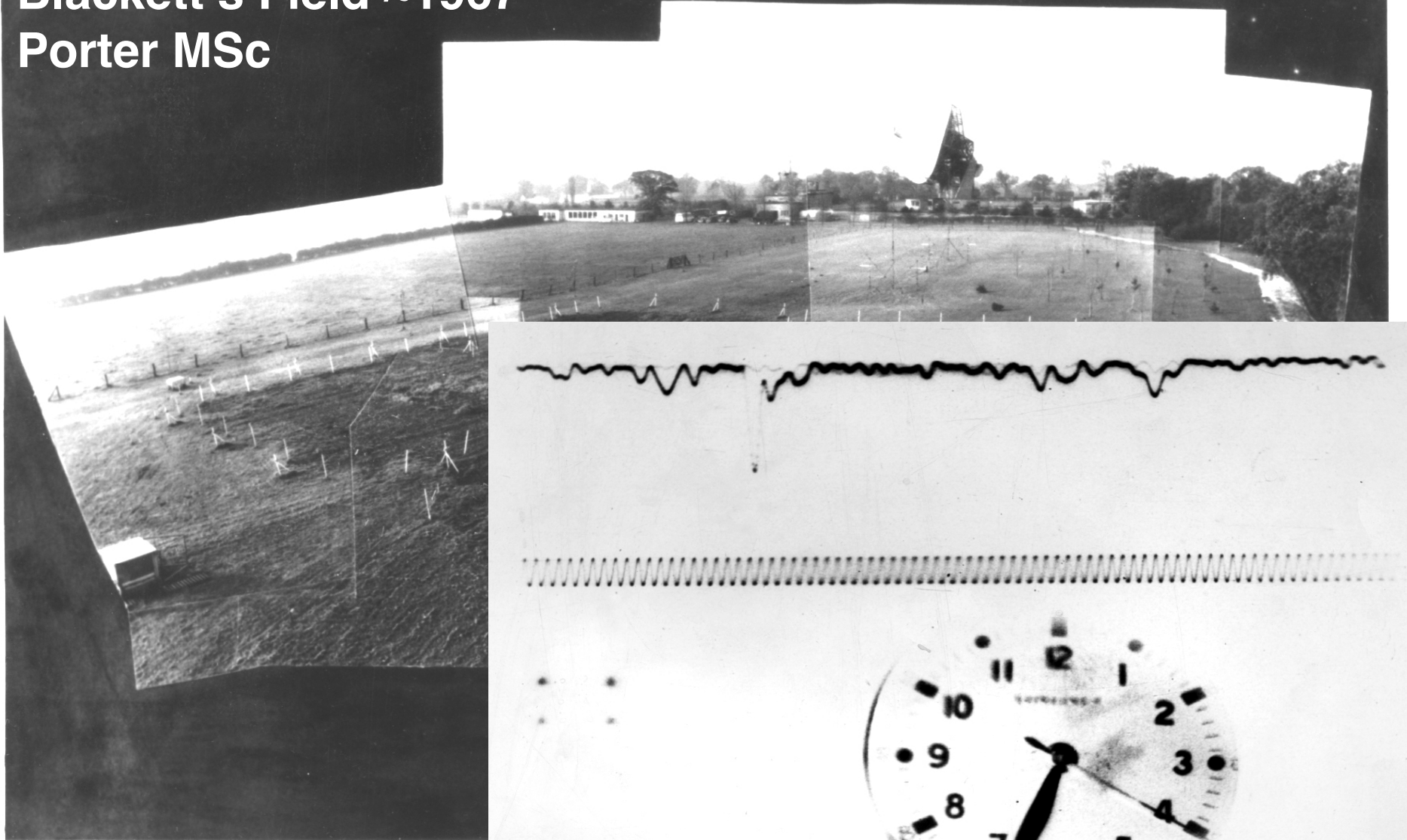
**Echos from meteor trails
Radio emission from M31**



**radio
astronomy**

First radio detection of air showers 1965

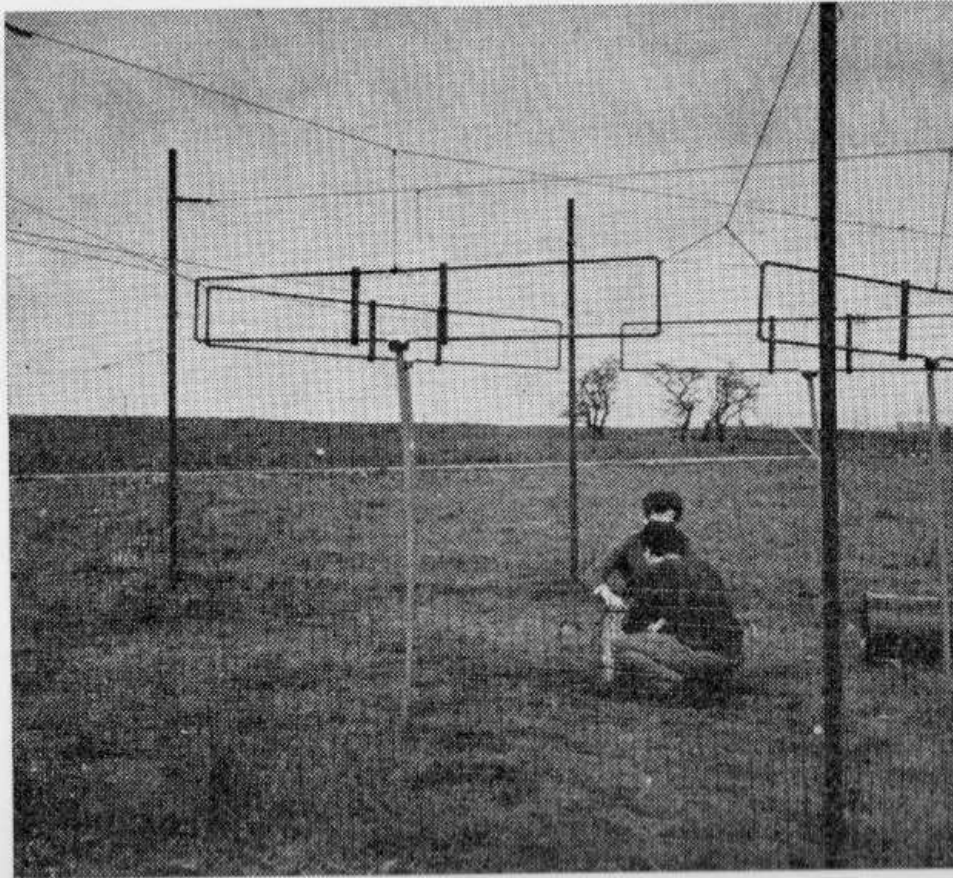
Blackett's Field ~1967
Porter MSc



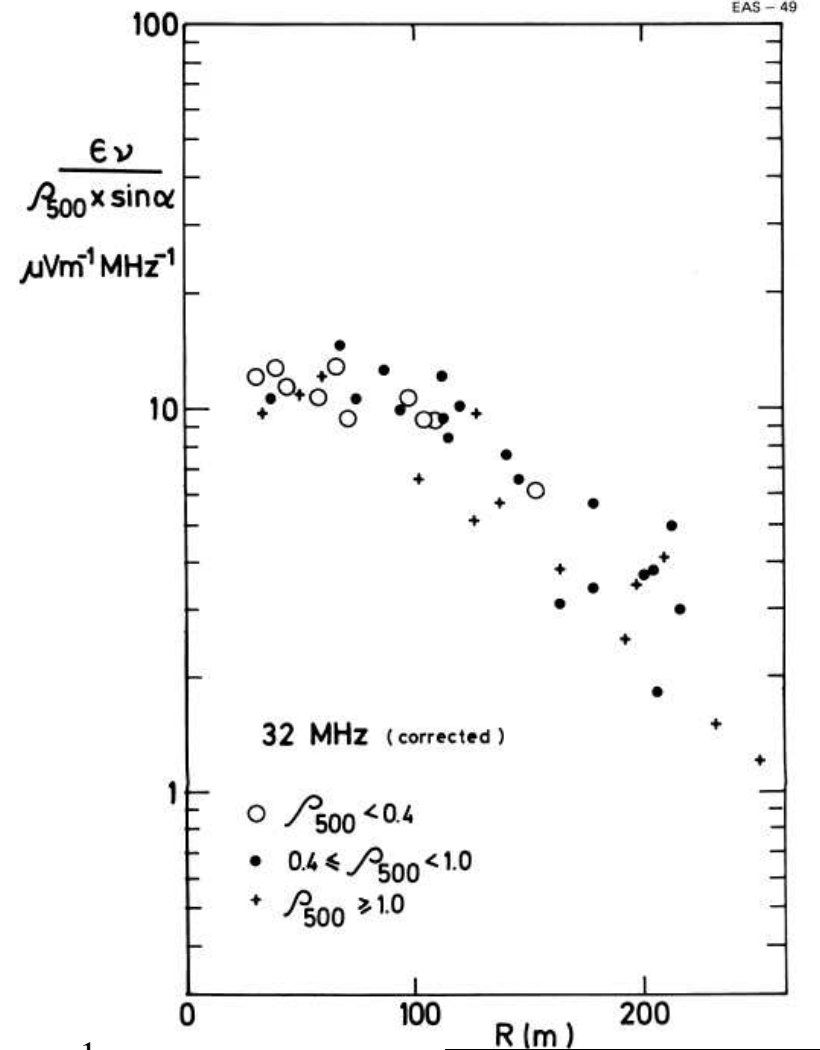
Jelley et al Nature 1965
R. A. Porter MSc Thesis 1967

Haverah Park (Leeds)

Allan 1971



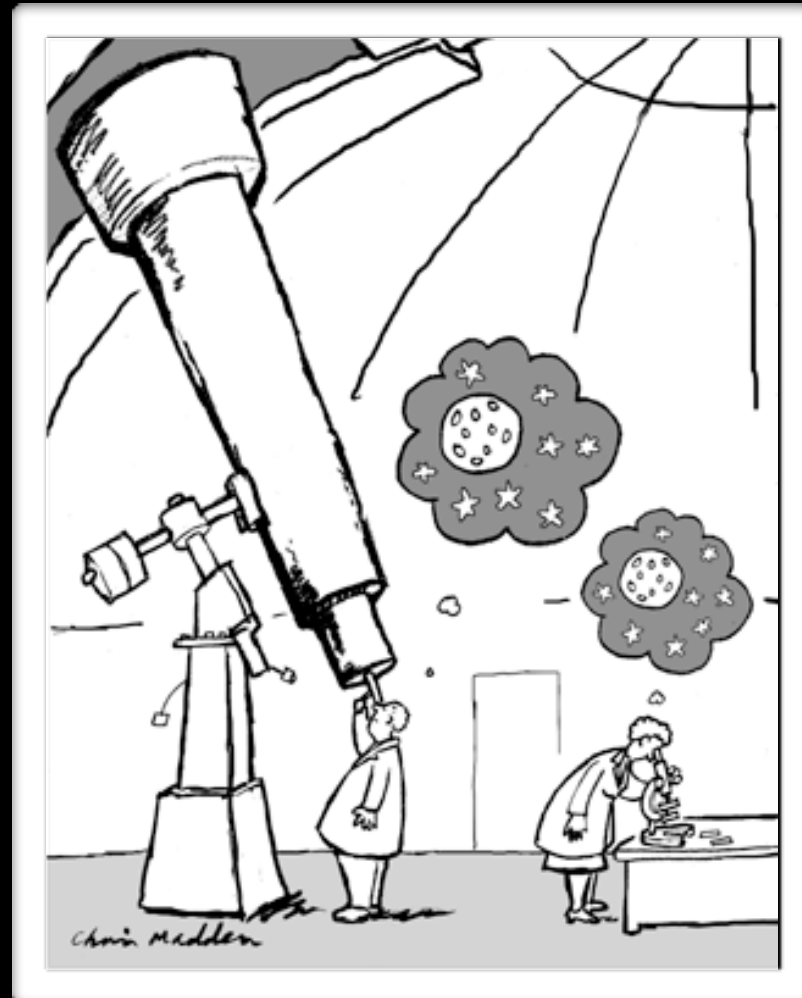
Recent receiving antennas (44 MHz) forming part of the Haverah Shower Array.



$$\epsilon_{\nu} = 2 \left(\frac{E_p}{10^{17}} \right) \left(\frac{\sin \alpha \cos \theta}{\sin 45 \cos 30} \right) \exp \left(\frac{-r}{r_0} \right) \left(\frac{\nu}{50} \right)^{-1} \mu\text{V/m/MHz}$$

$r_0 = 110$ m at $\nu = 55$ MHz. $\alpha =$ angle to B, $\theta =$ Zenith angle

Radio Detectors



Large-scale radio detectors to measure extensive air showers



0.5 km²



CODALEMA 0.5 km²



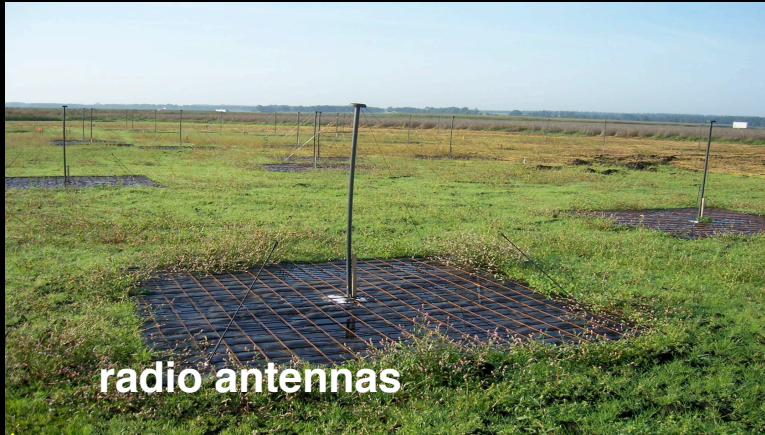
**5 km² (core)
~1800 antennas**



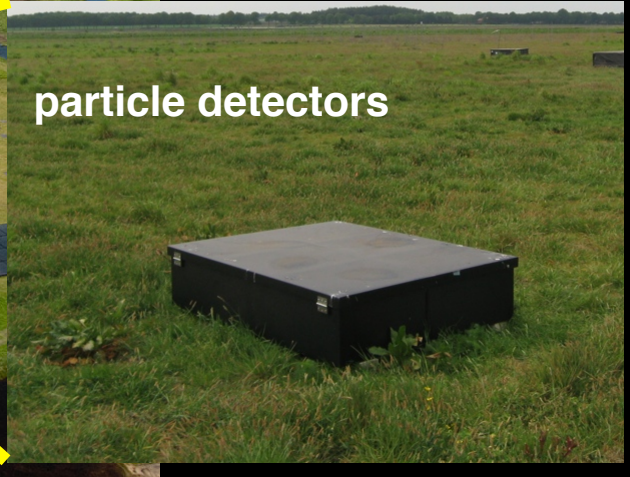
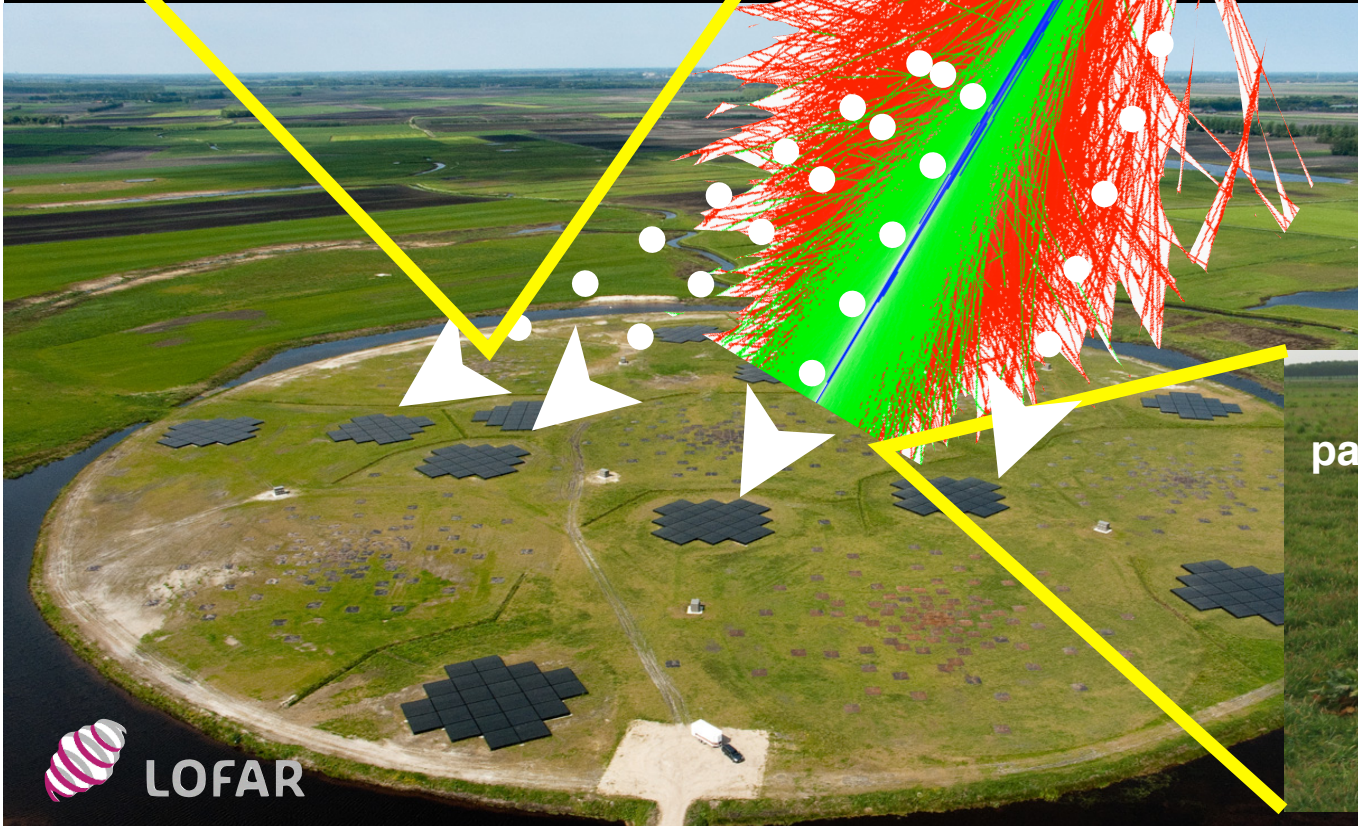
**20 km²
~160 antennas**



**next-
generation
cosmic-ray
detector
20 000 km²**



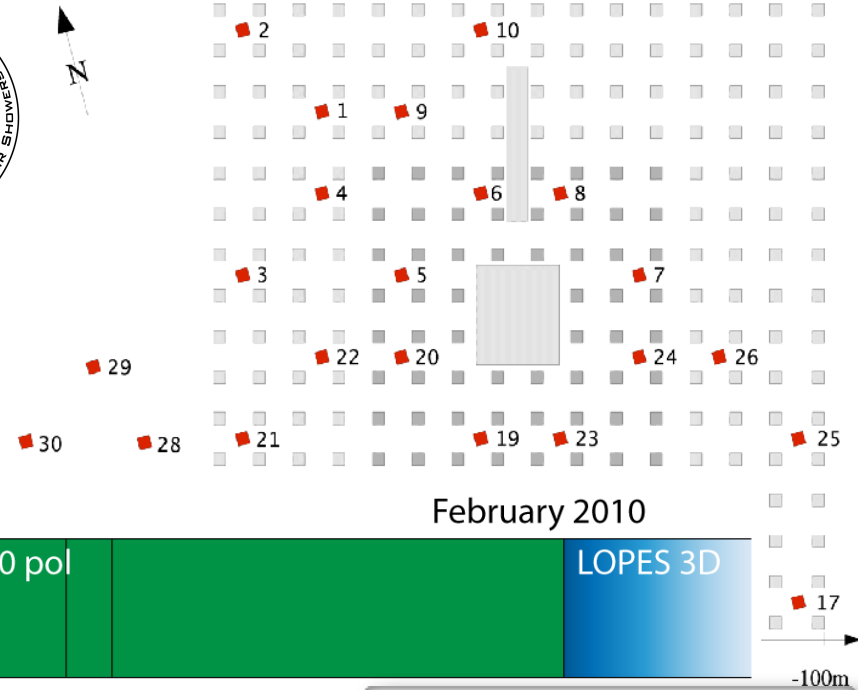
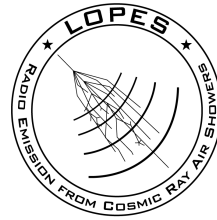
- Objectives:**
- understand radio emission processes
 - measure properties of cosmic rays
 - energy
 - mass
 - direction



LOPES

Lofar Prototype Station

30 antennas operating at
KASCADE-Grande

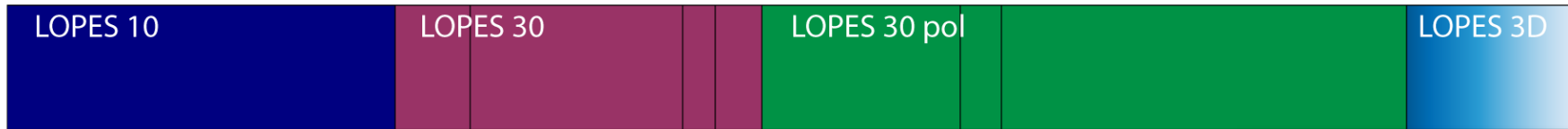


April 2003

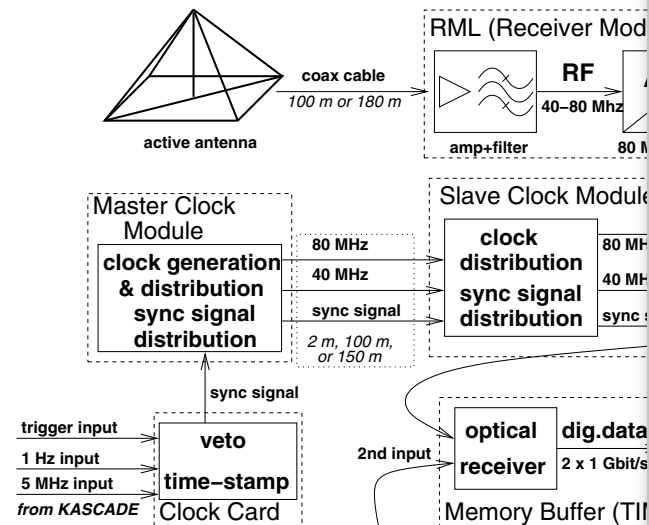
February 2005

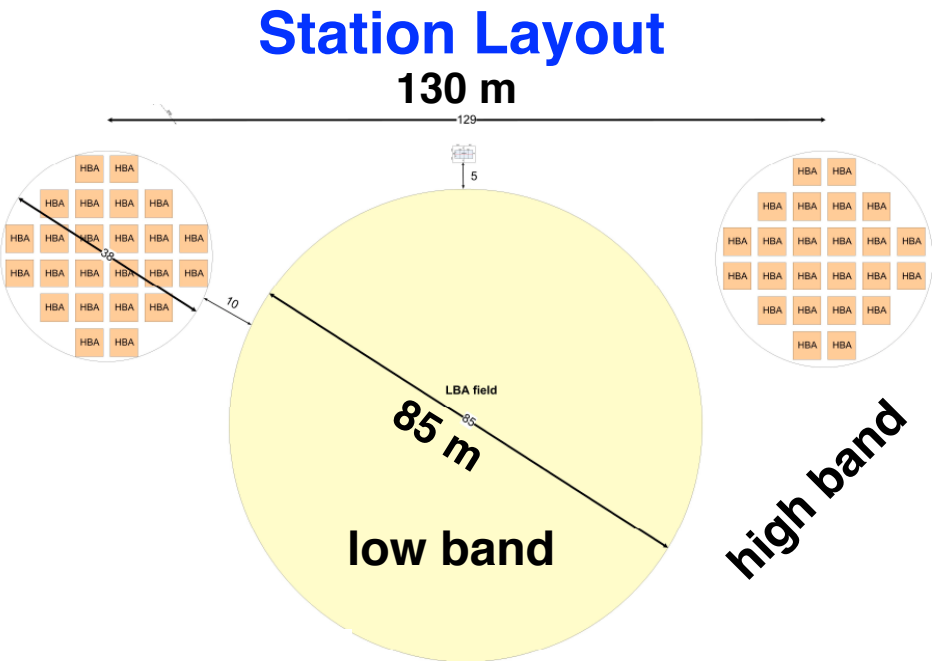
December 2006

February 2010



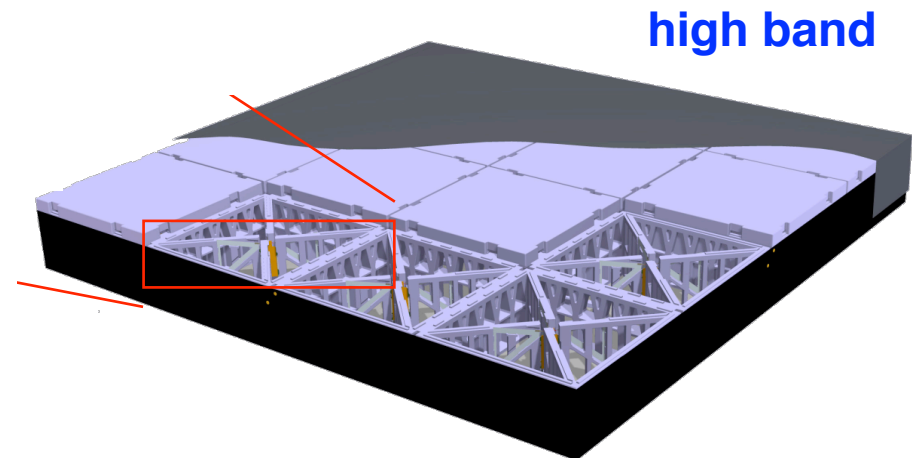
digital radio interferometry





each (dutch) station:

96 low-band antennas **30- 80 MHz**
high-band antennas (2x24 tiles) **120-240 MHz**



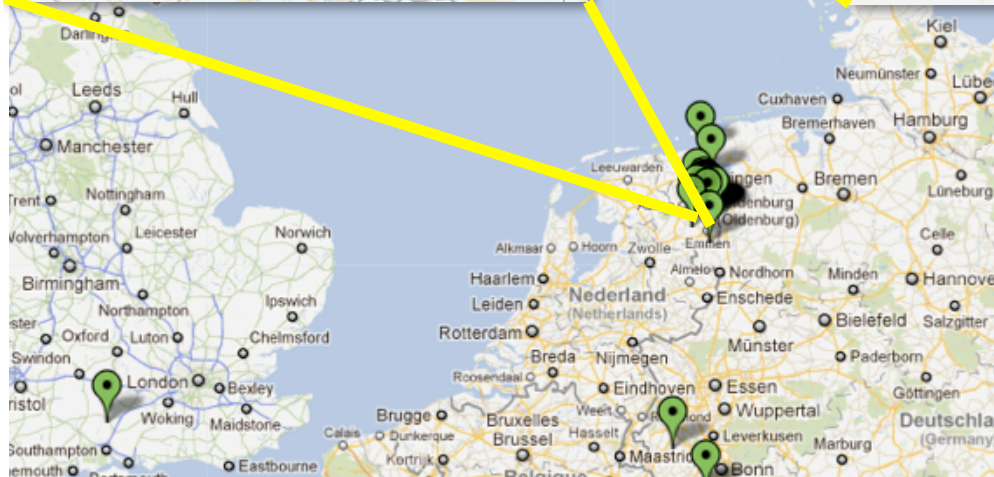
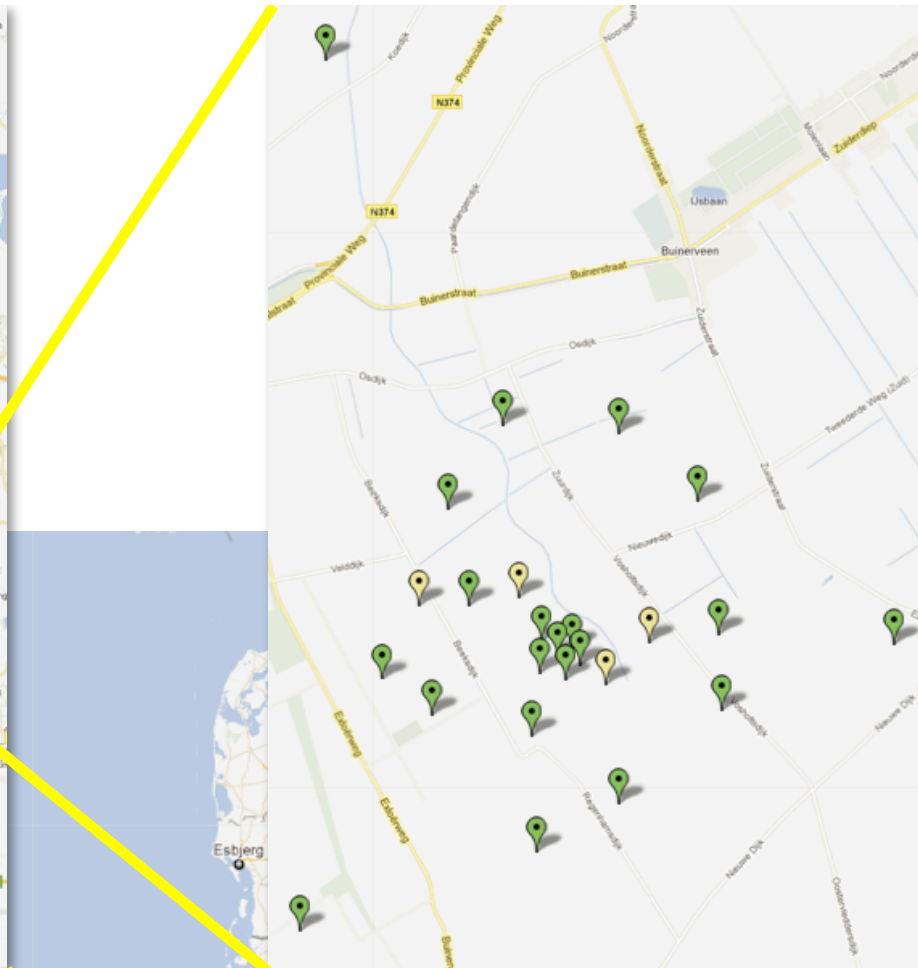
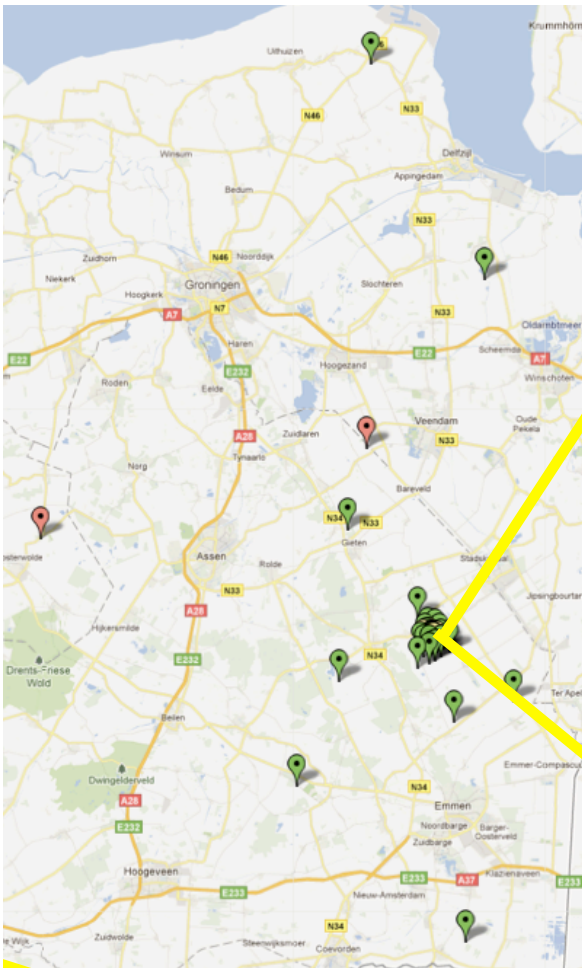
www.lofar.org

LOFAR stations across Europe



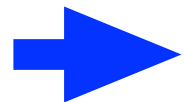
**Dense core
in NL**

**18 stations
~ 5 km²**

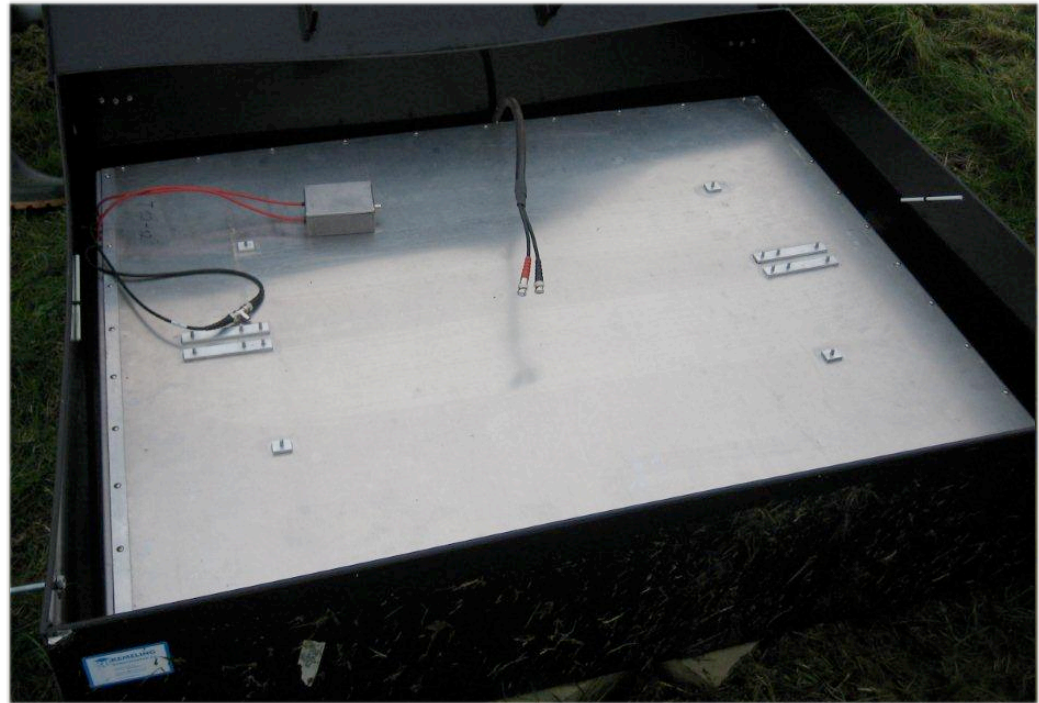


LOFAR Radboud Air Shower Array - LORA

20 scintillator units
($\sim 1 \text{ m}^2$ each)
read out by
wavelength shifter
bar and PMT
in LOFAR core

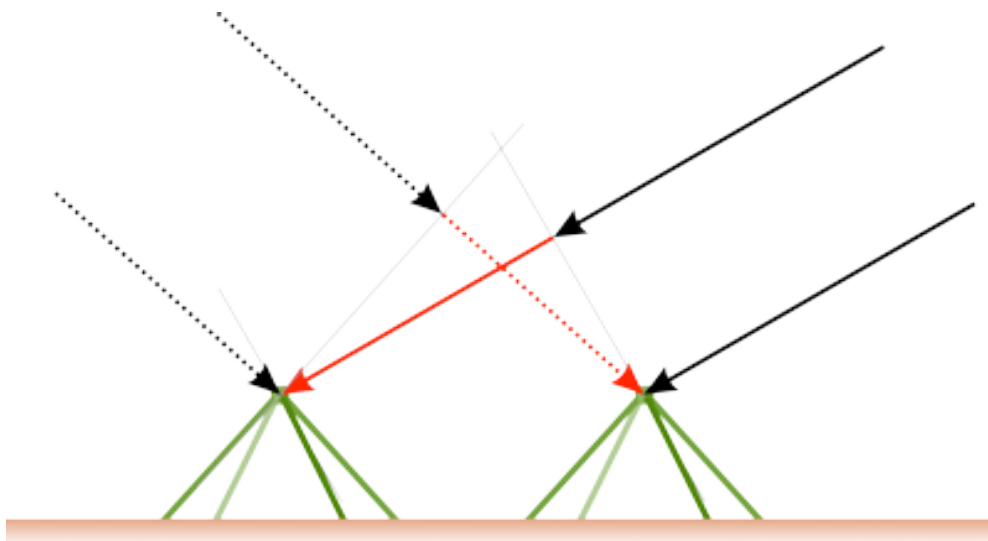
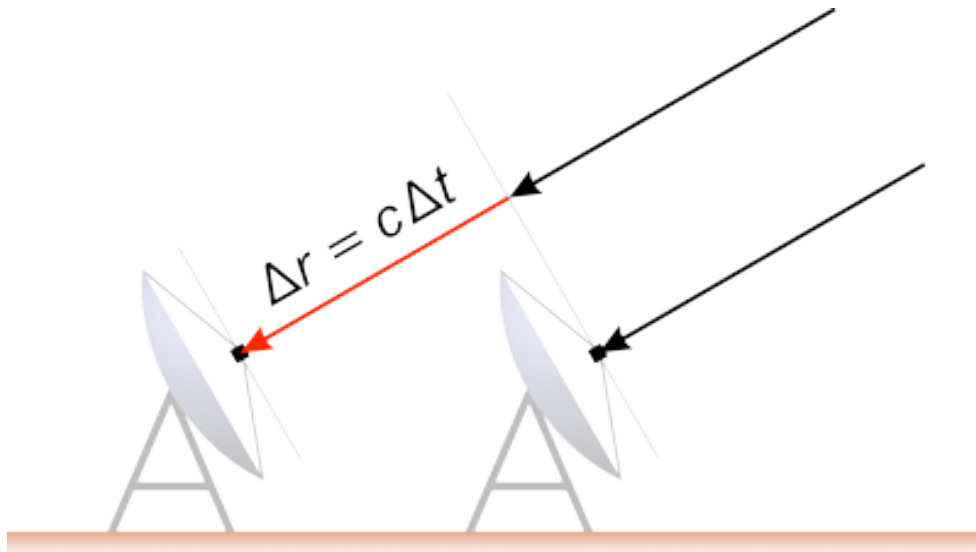
 provide

- properties of EAS
- and trigger

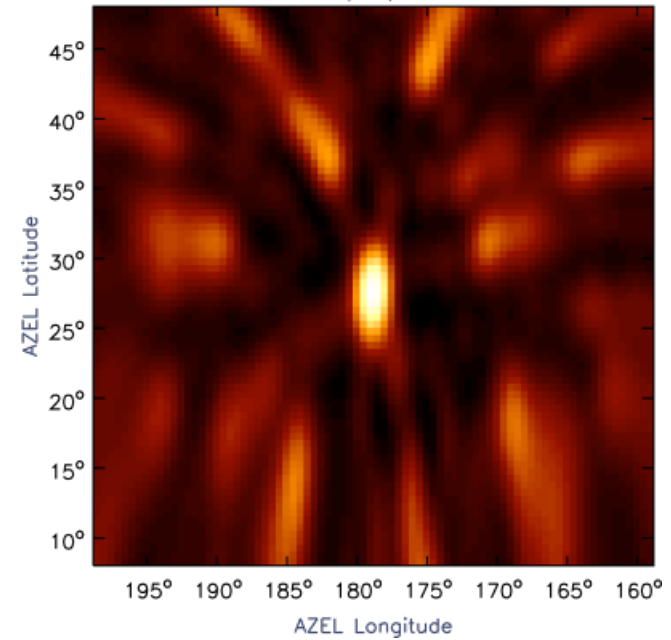


LOFAR

Digital beam forming



Solar burst, 2003/10/28, 11:05:49.000

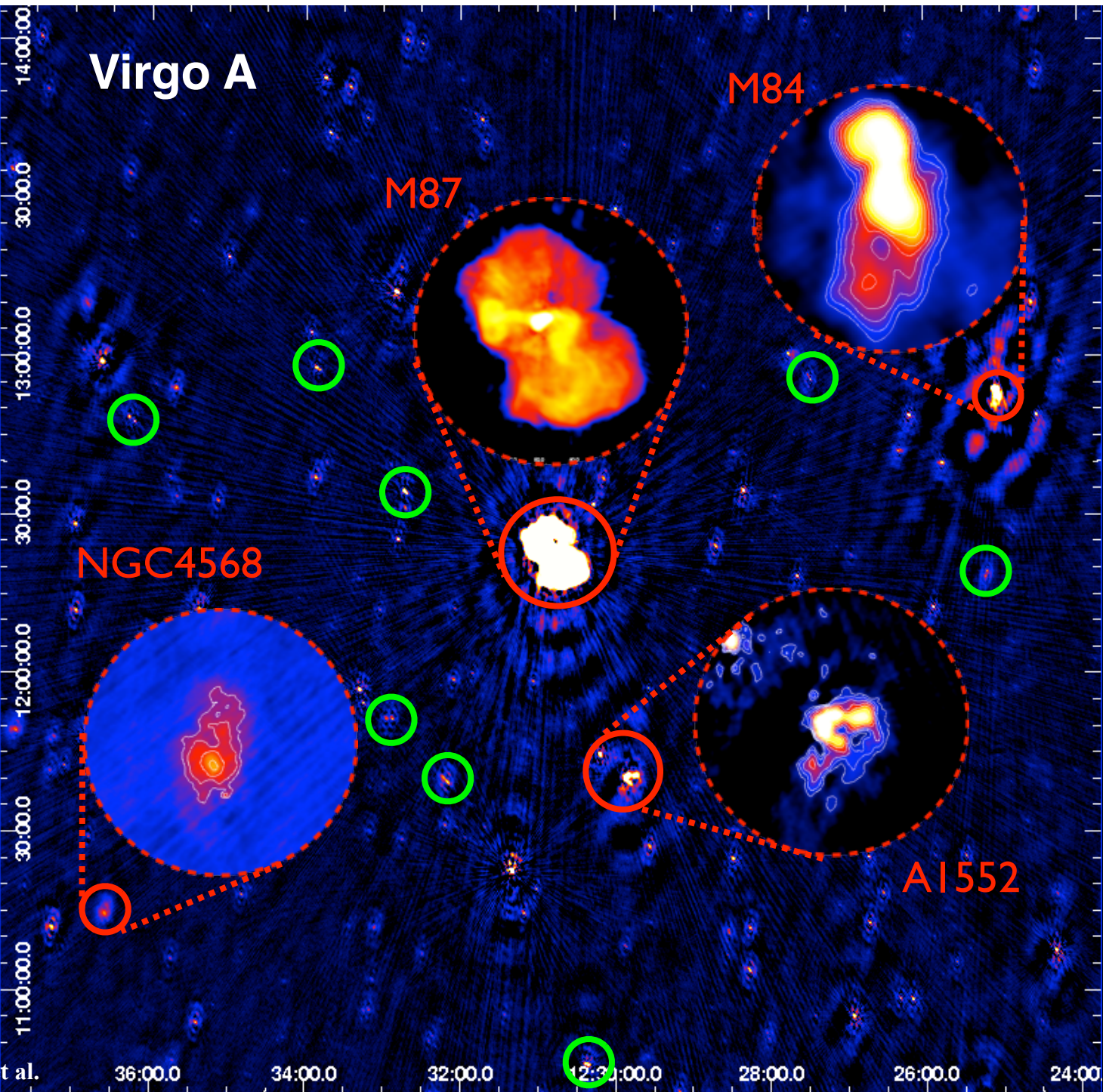


Solar burst observed with LOPES



IBM Blue Gene Supercomputer

Virgo A



de Gasperin et al.

36:00.0

34:00.0

32:00.0

30:00.0

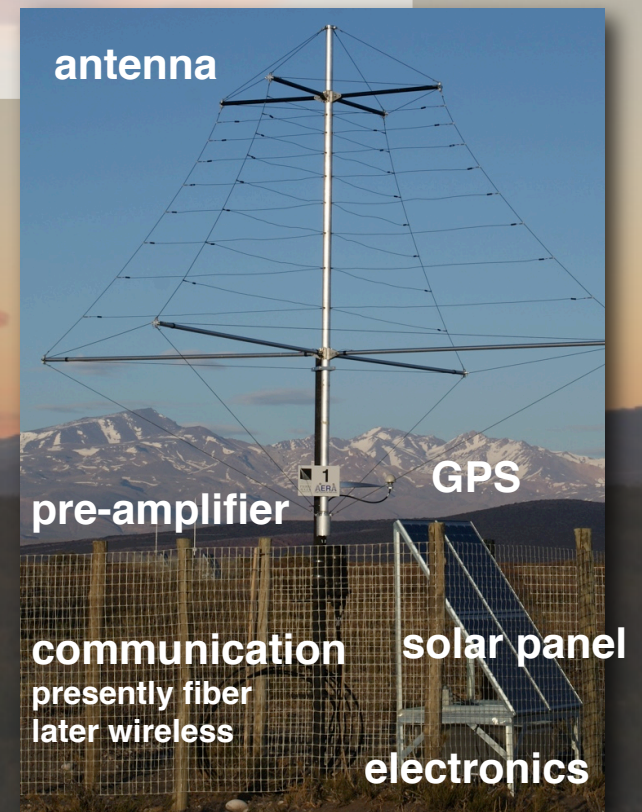
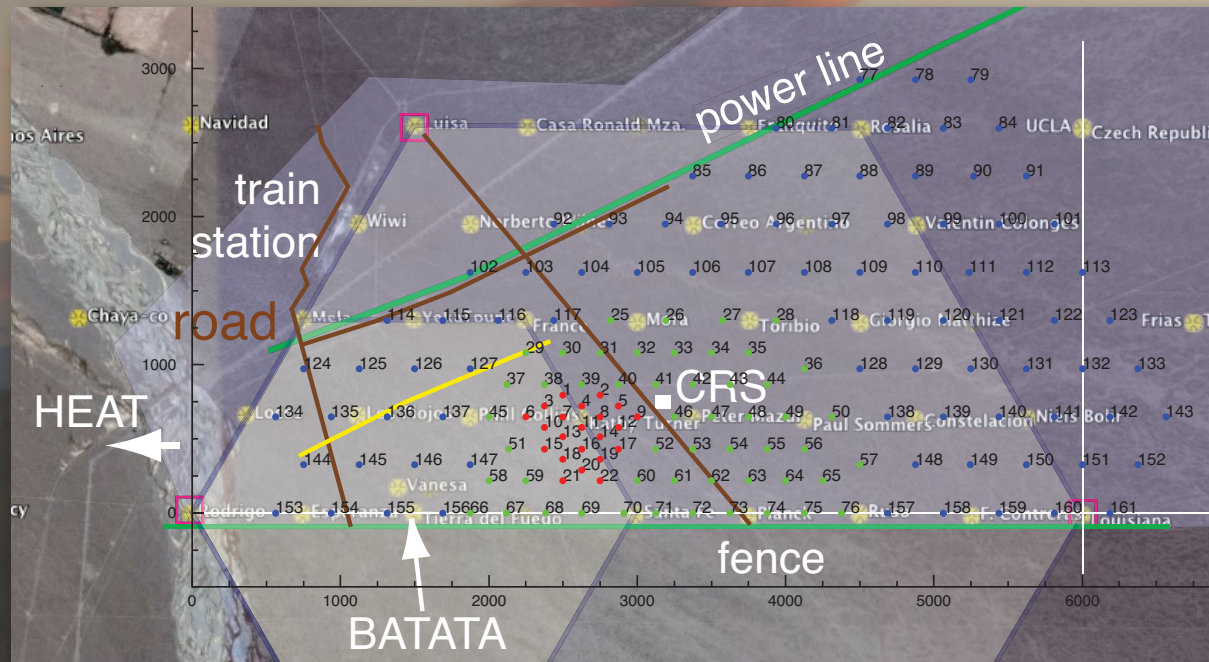
28:00.0

26:00.0

24:00.0

Objective:

- measure radio emission from EAS in frequency range 30 MHz - 80 MHz
- ~20 km² array with ~160 antennas
- operation together with infill/HEAT/AMIGA
- three antenna spacings to cover efficiently $17.2 < \lg E/eV < 19.0$
- measure composition of cosmic rays in energy region of transition from galactic to extragalactic cosmic rays





geomagnetic field

air shower

comms antenna

GPS antenna

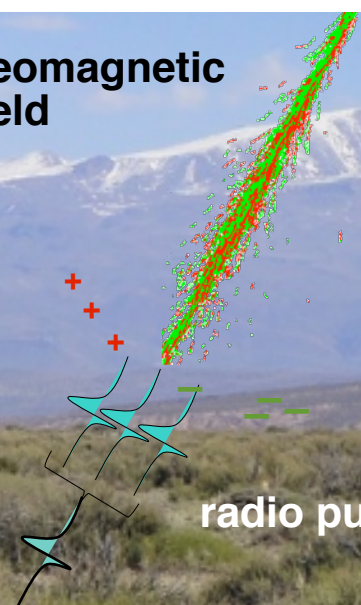
radio pulses

physics antenna

30 - 80 MHz

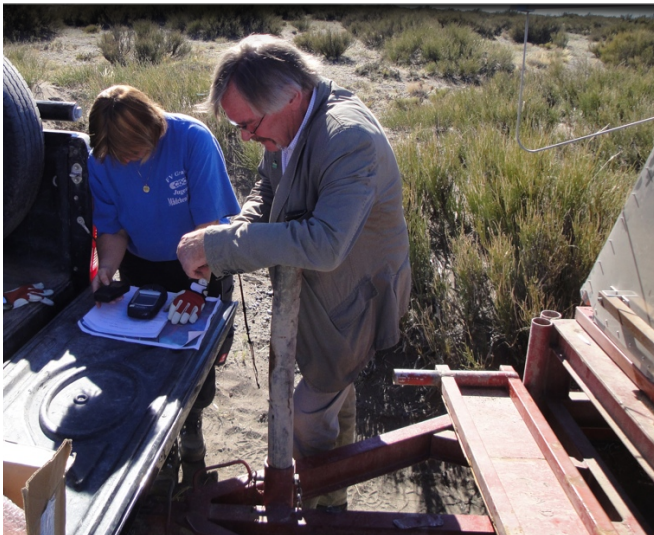
solar panel

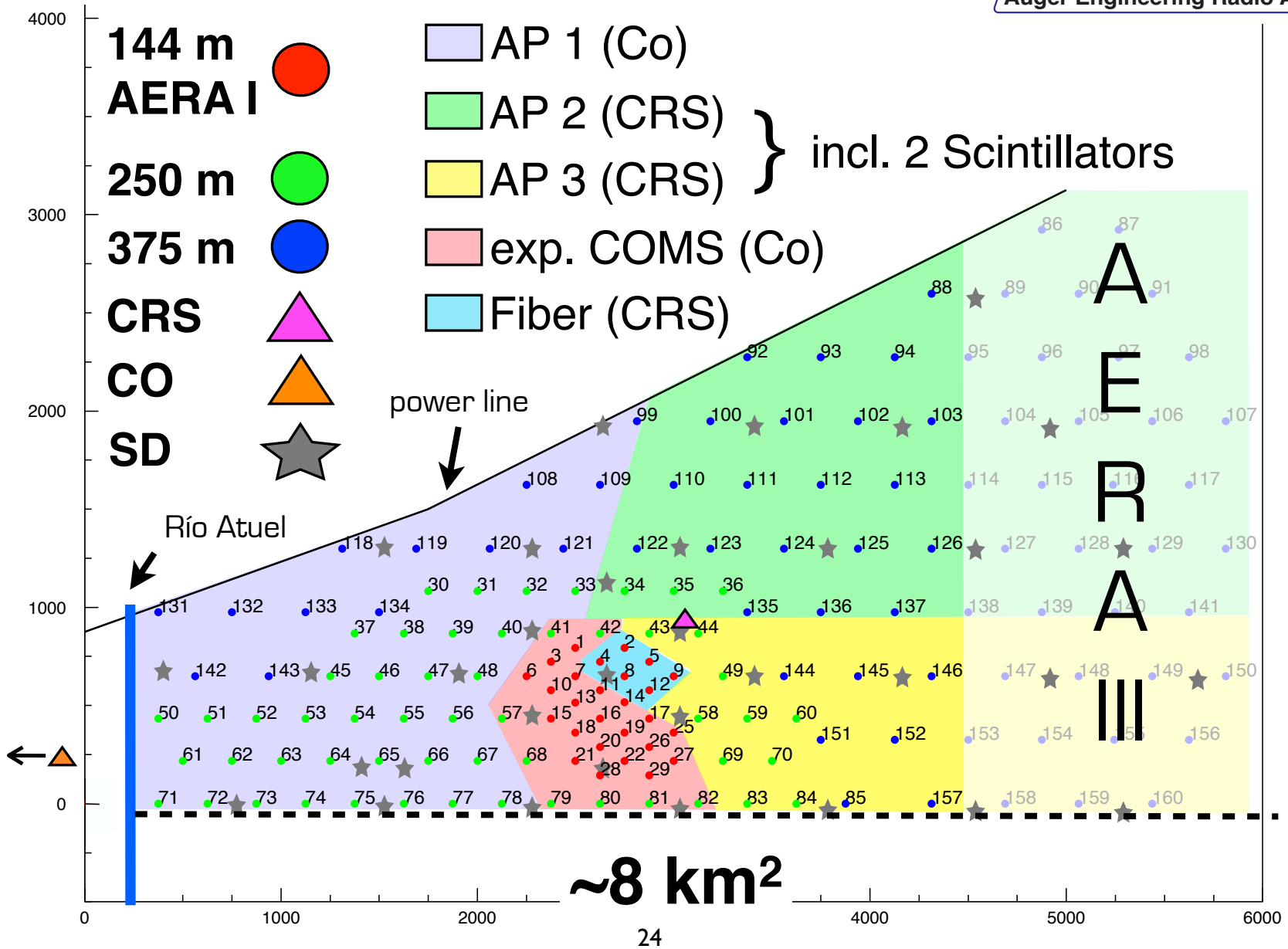
electronics & battery

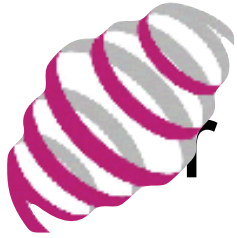


68
AERA

installation







LOFAR

high antenna density:
precision measurements
of radio emission

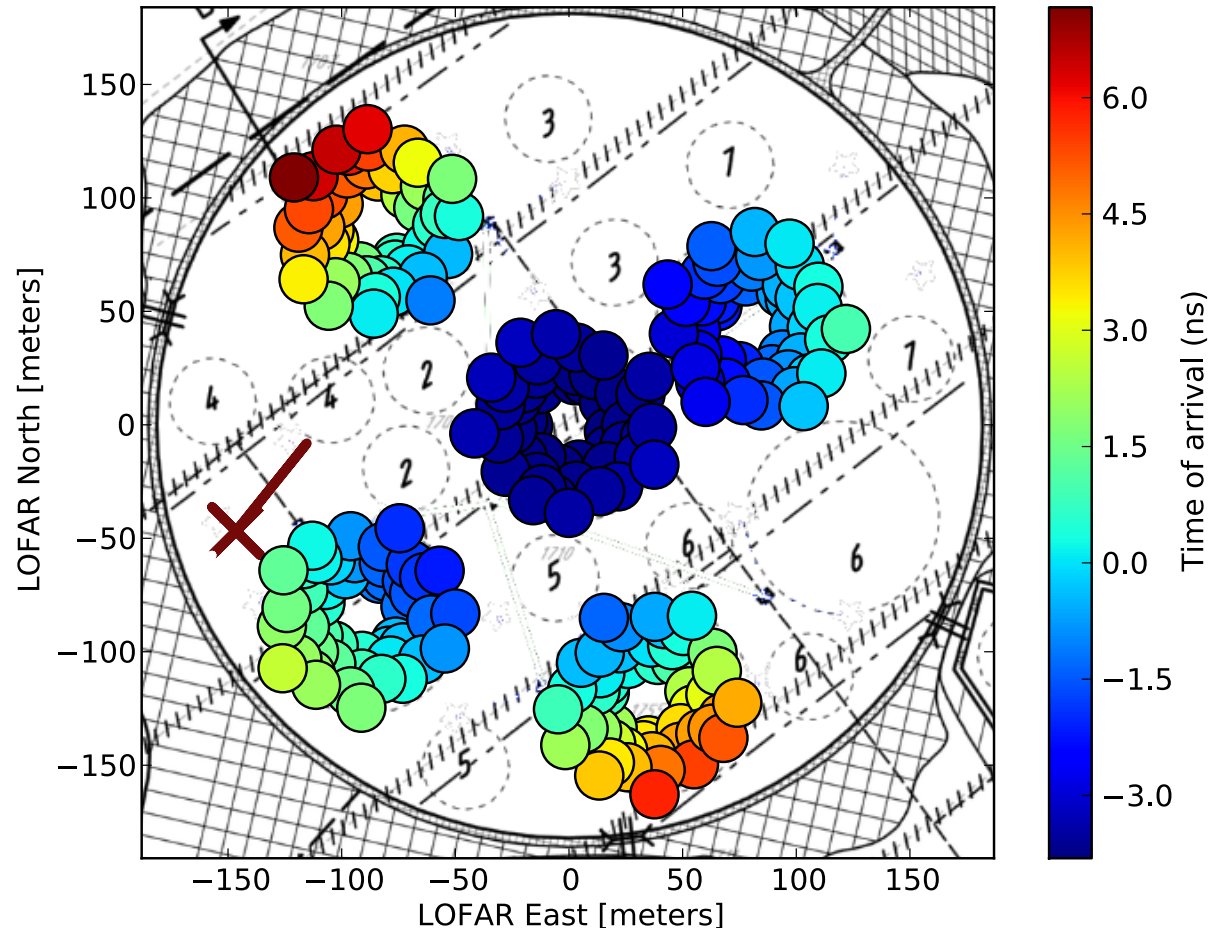
Ability of LOFAR to measure shape of shower front

LOFAR can resolve 2 ns (no additional phase calibration)

Simulated spherical shower front for measured air shower signals

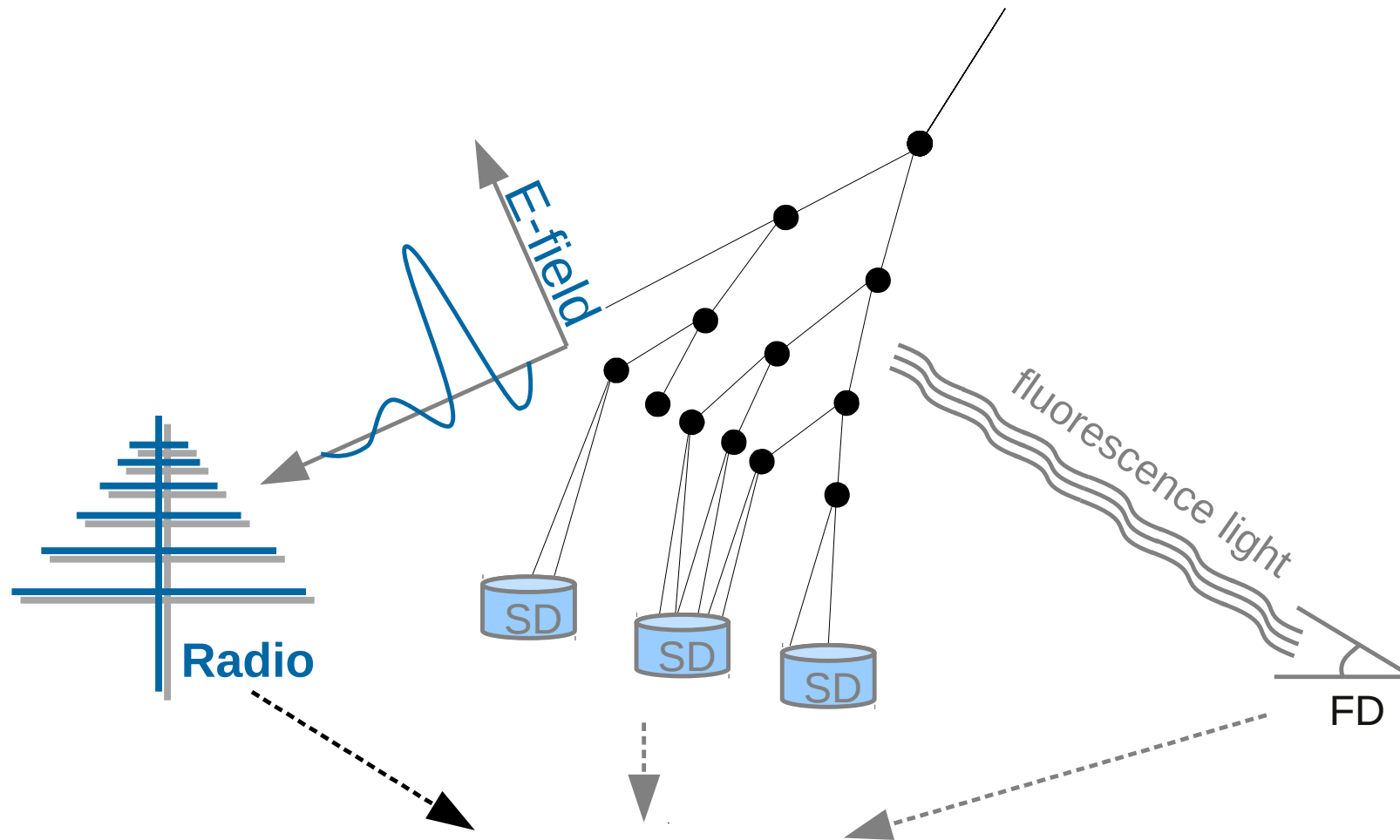
Differences in time with respect to plane wave are resolvable

Deviations from plane wave
Simulated wavefront curvature, $R = 4$ km





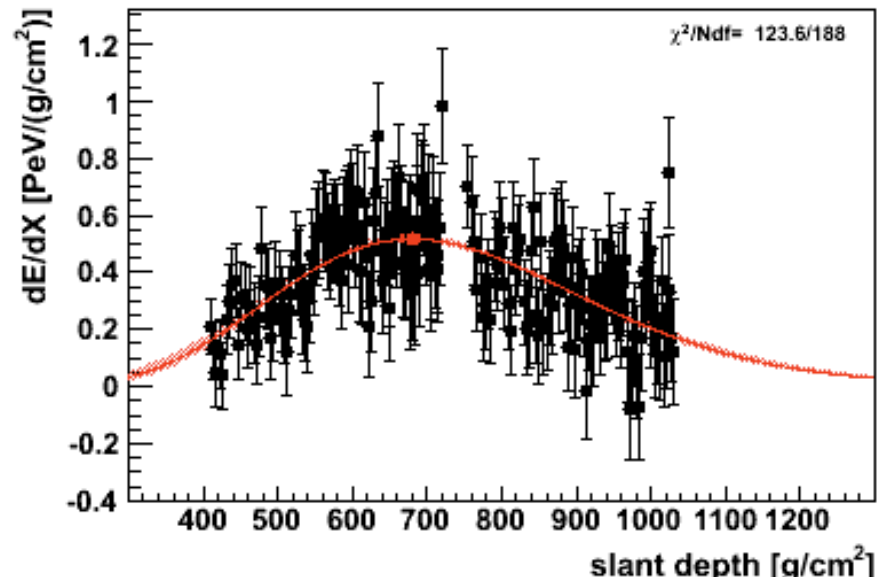
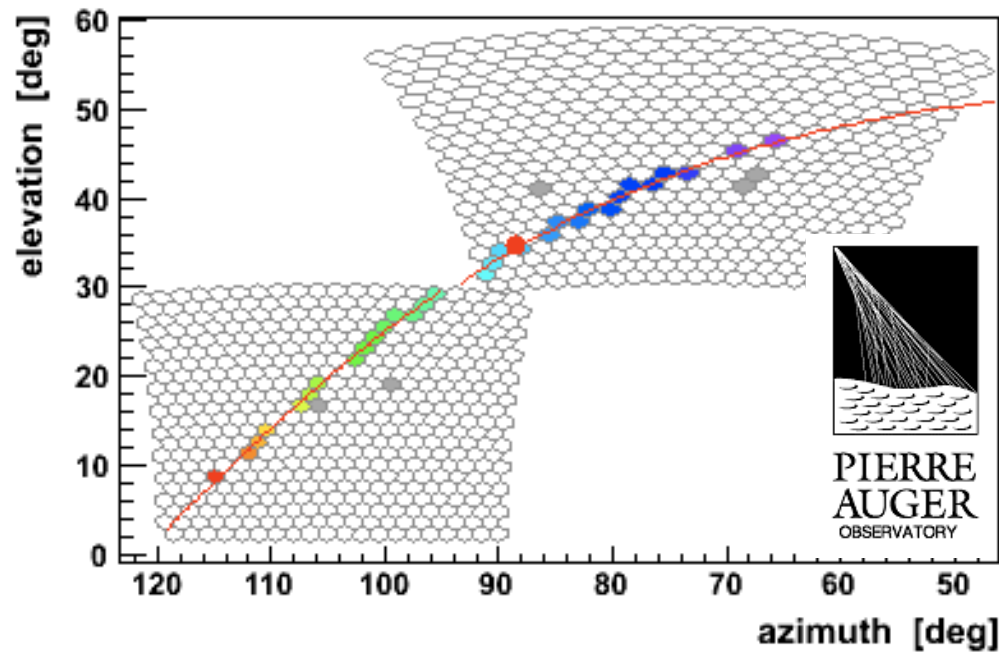
**complementary techniques to observe
air showers:
cross calibration between techniques**



shower properties: energy, mass, direction

Air shower measured in

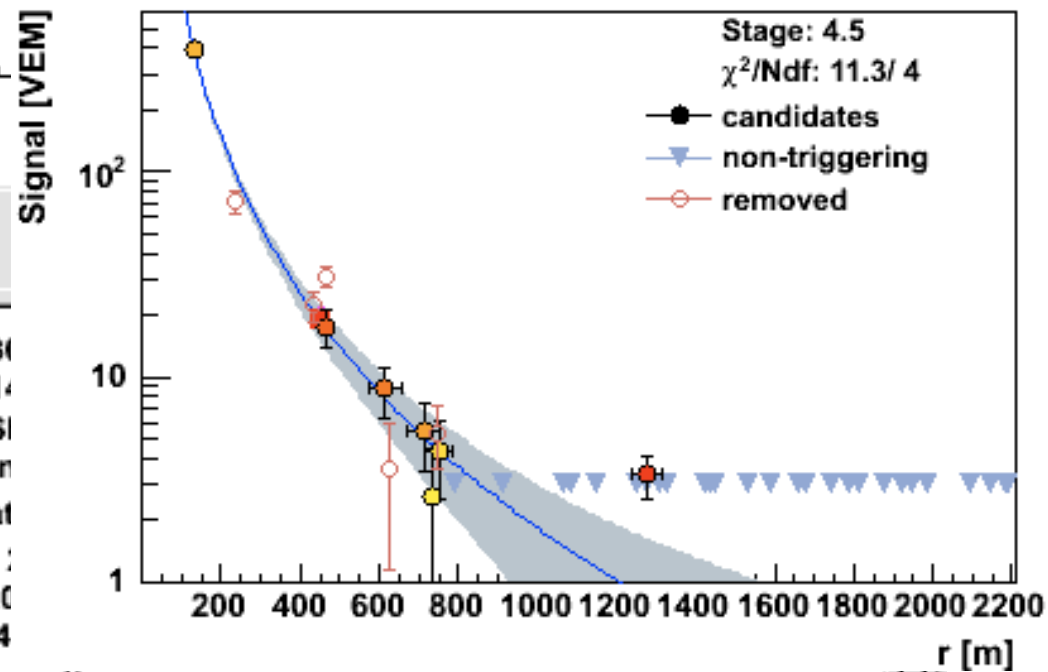
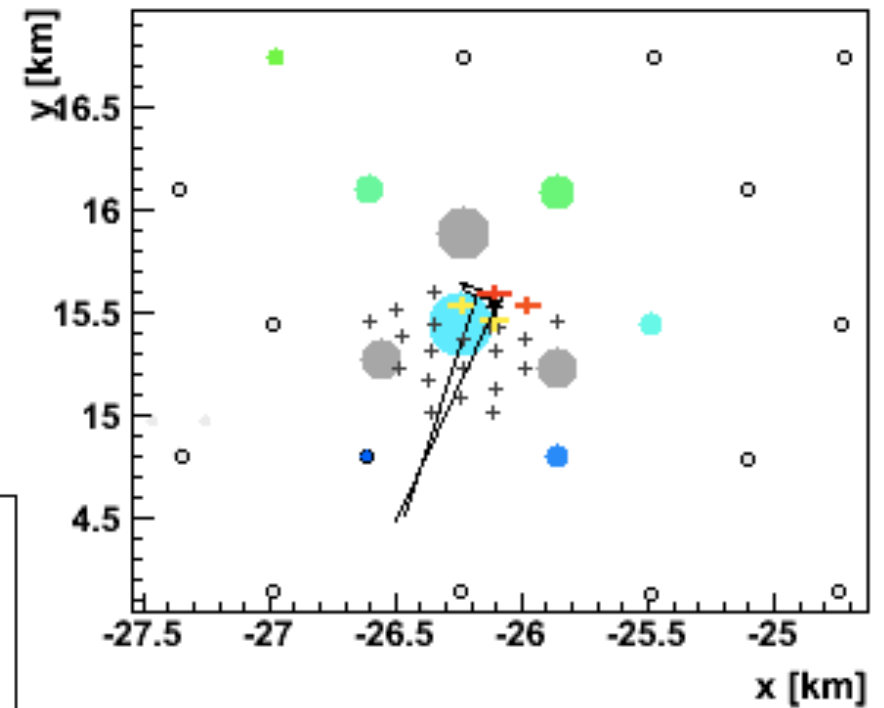
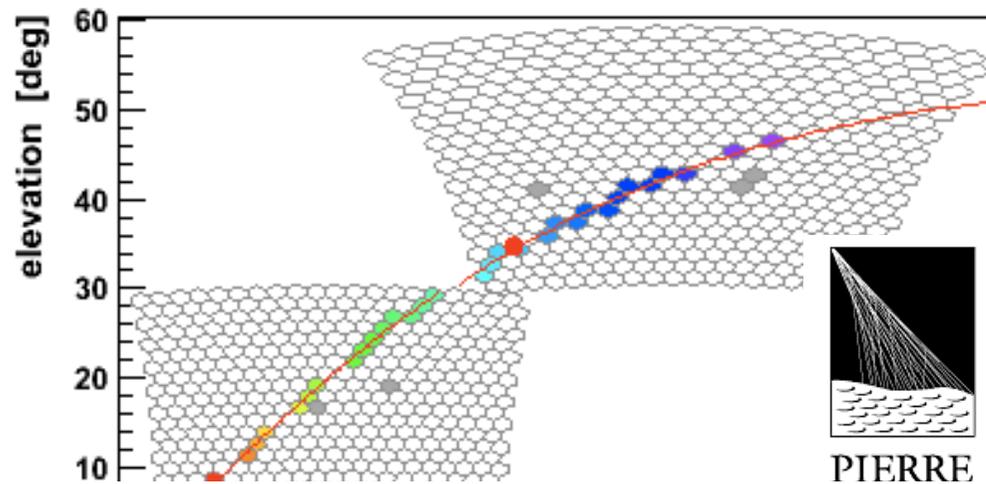
fluorescence light



Air shower measured in

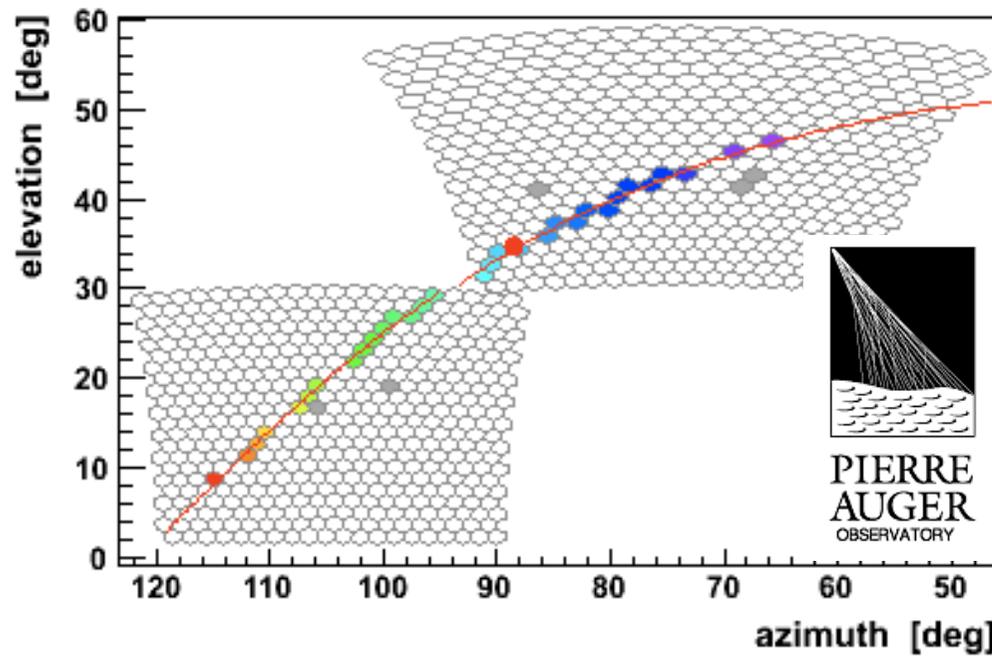
fluorescence light

water Cherenkov detectors

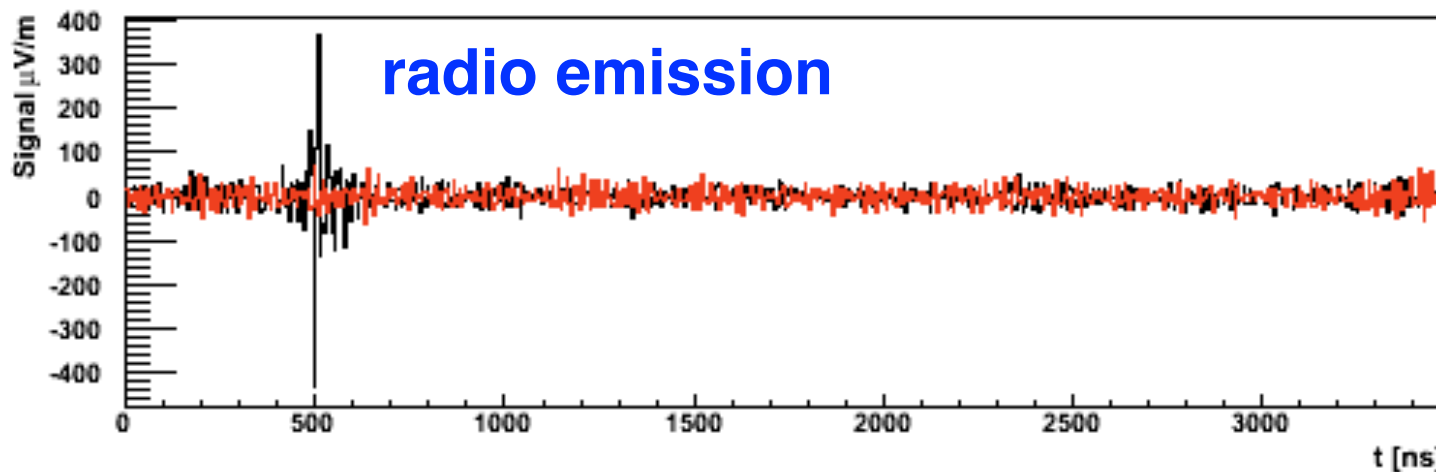
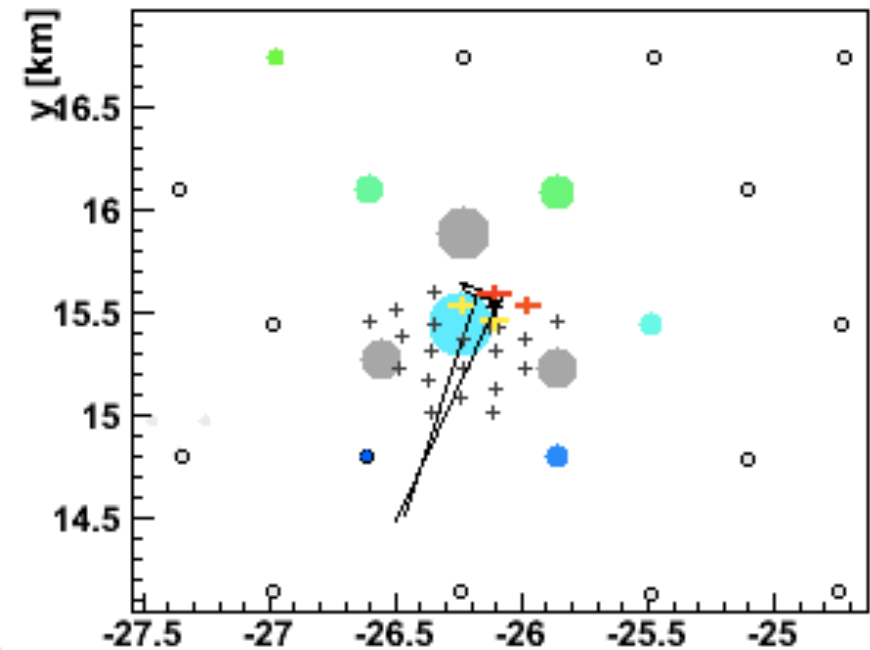


Air shower measured in

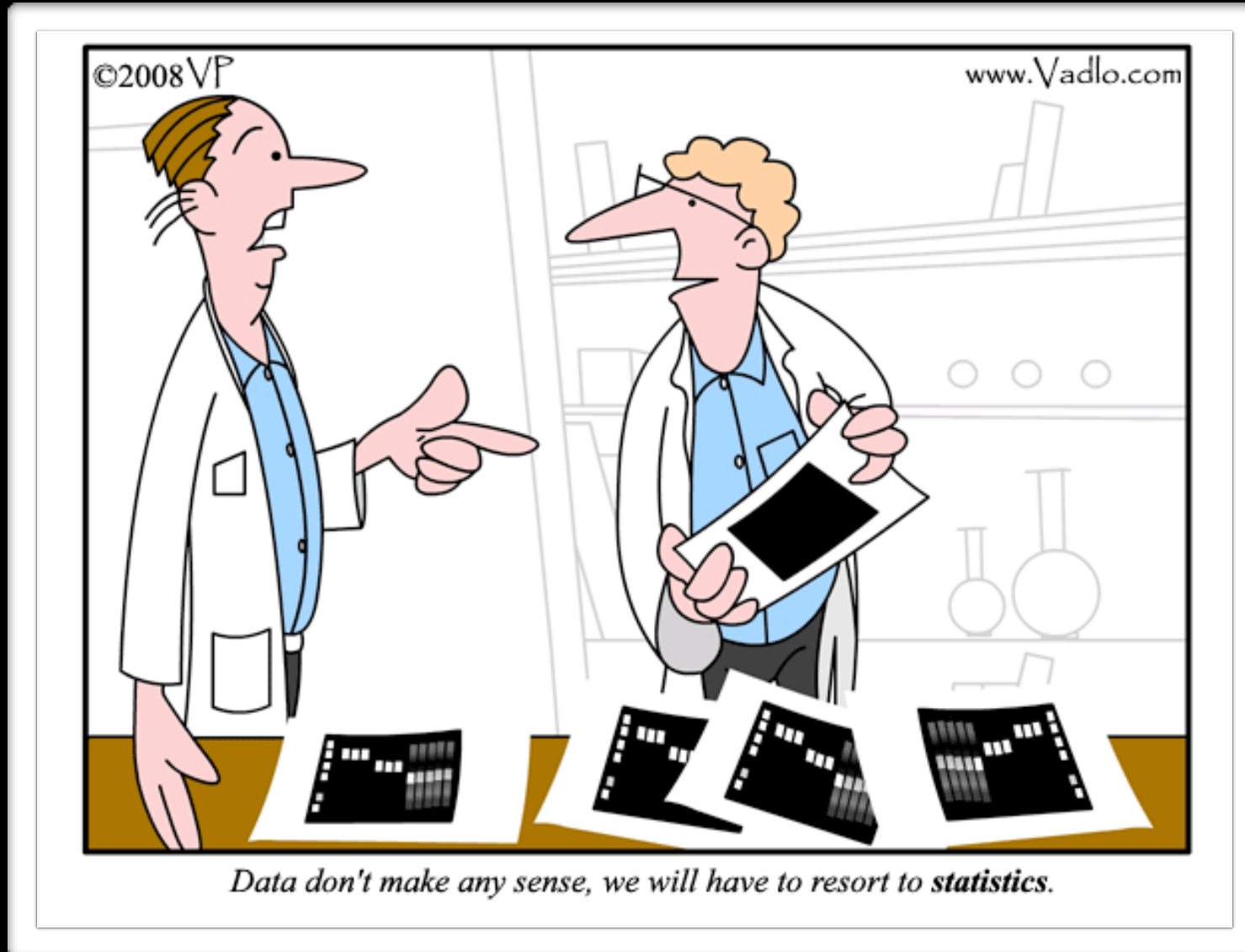
fluorescence light



water Cherenkov detectors

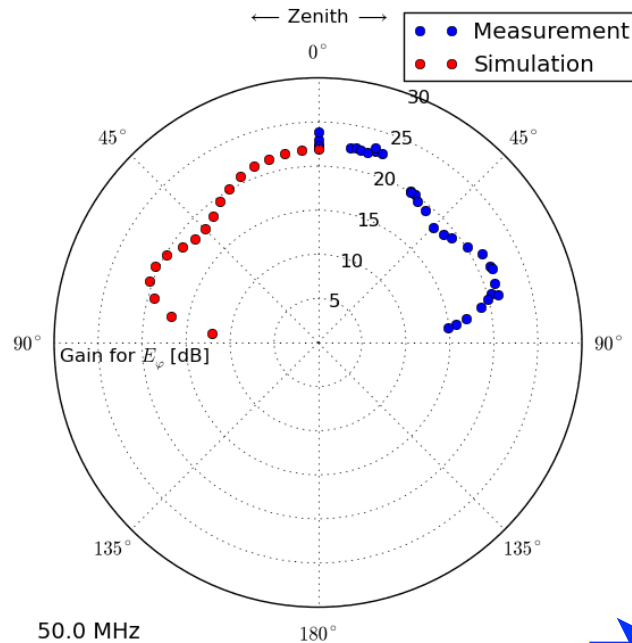
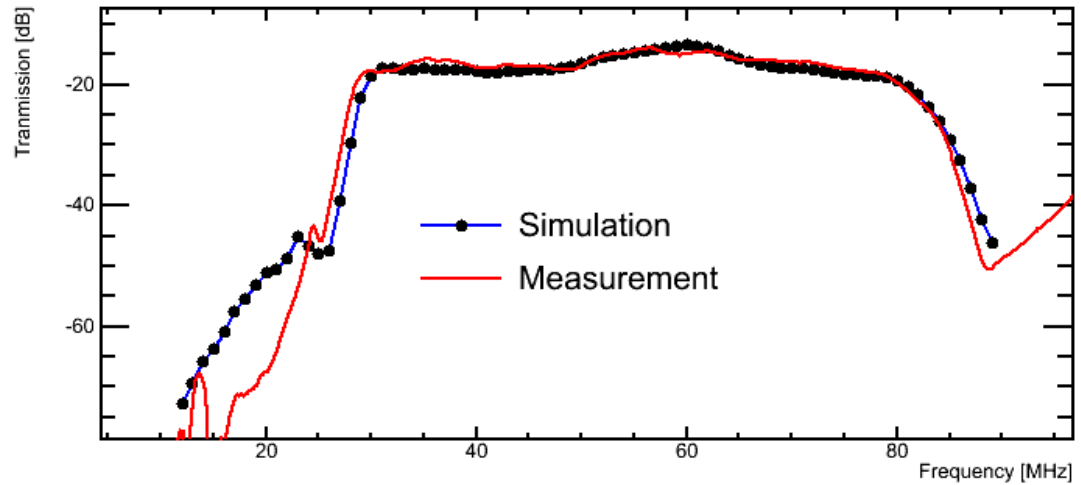


Calibration & Data Analysis

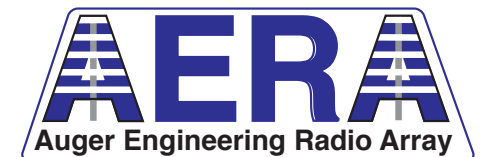


In-situ calibration

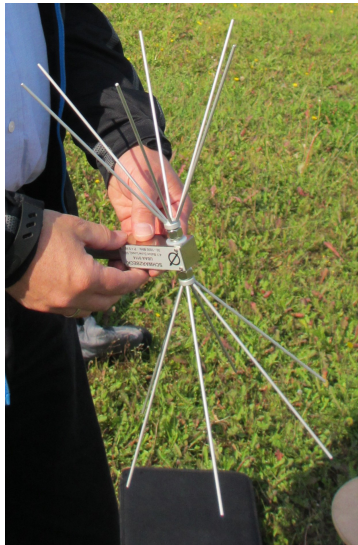
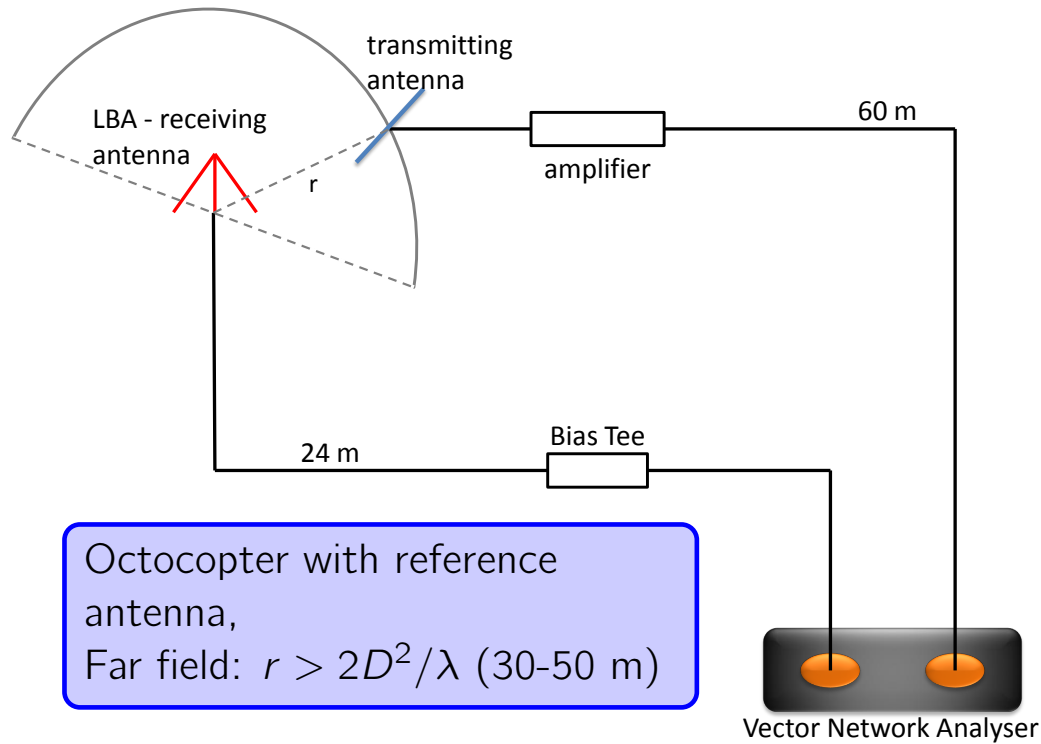
frequency dependent antenna gain



horizontal gain



In-situ calibration of the antennas





In-situ calibration of the antennas

Friis transmission equation

$$\frac{P_r}{P_t} = \left(\frac{\lambda}{4\pi R} \right)^2 G_r G_t$$

P_r - Power of receiver

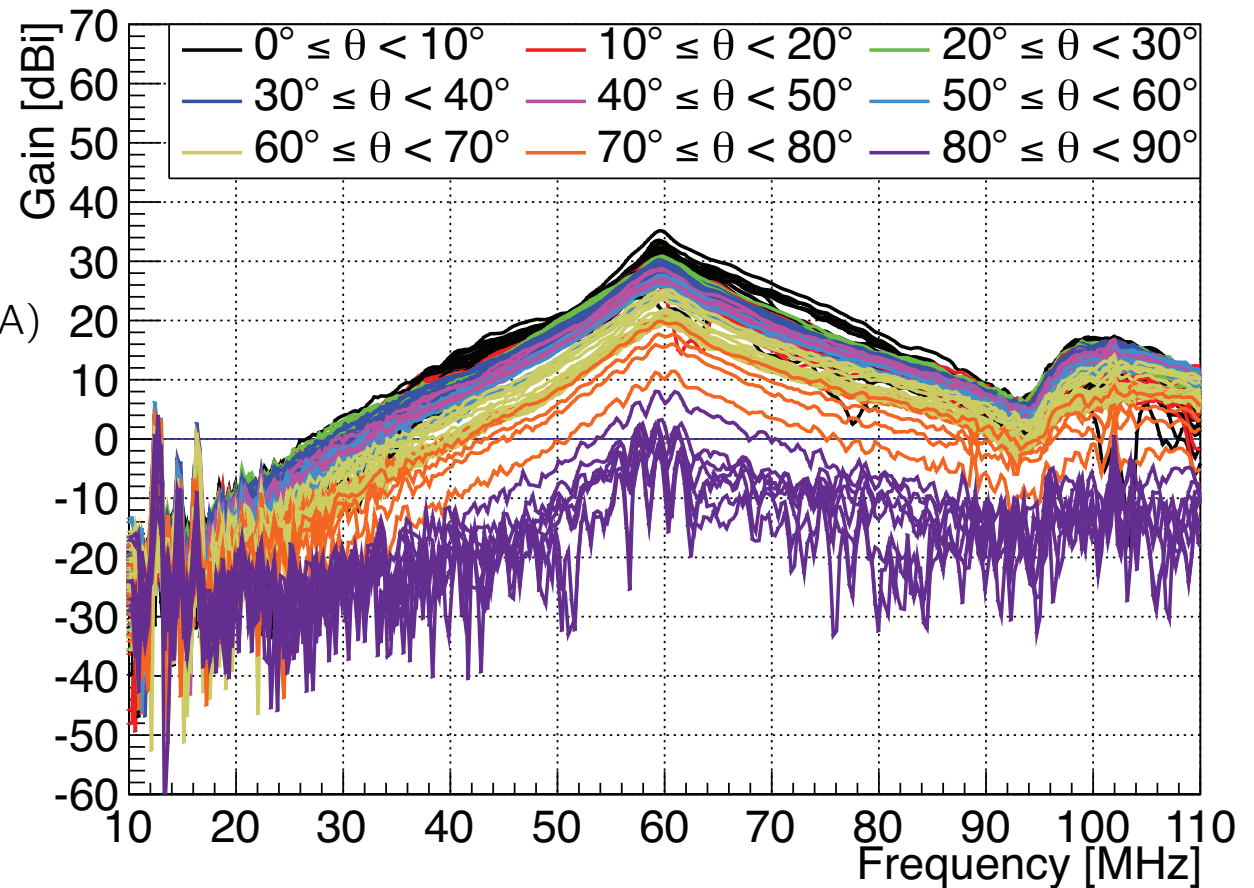
P_t - Power of transmitter

λ - Wavelength

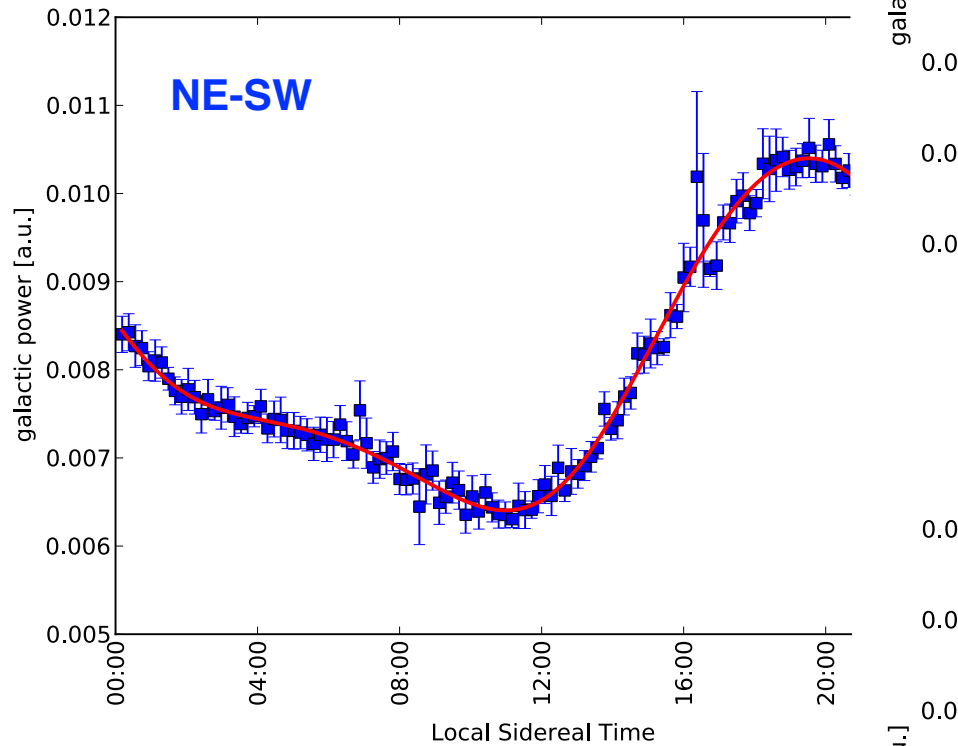
G_t - Gain of transmitting antenna

R - Distance between antennas

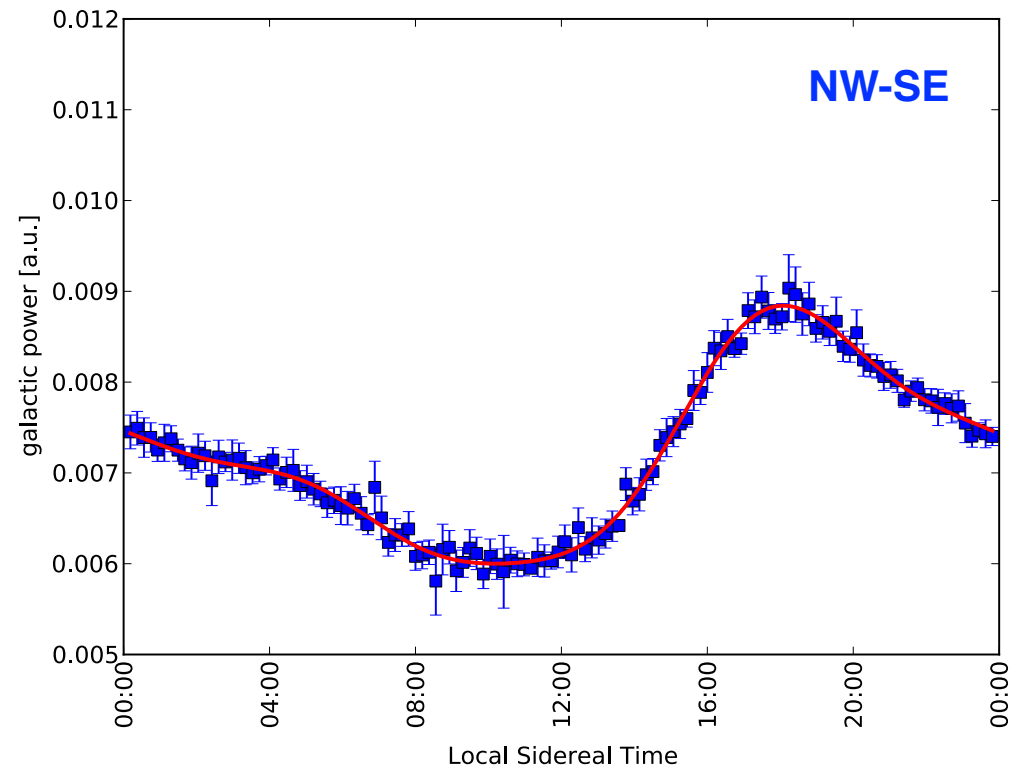
G_r - Gain of receiving antenna (LBA)



Integrated spectral power vs. local siderial time

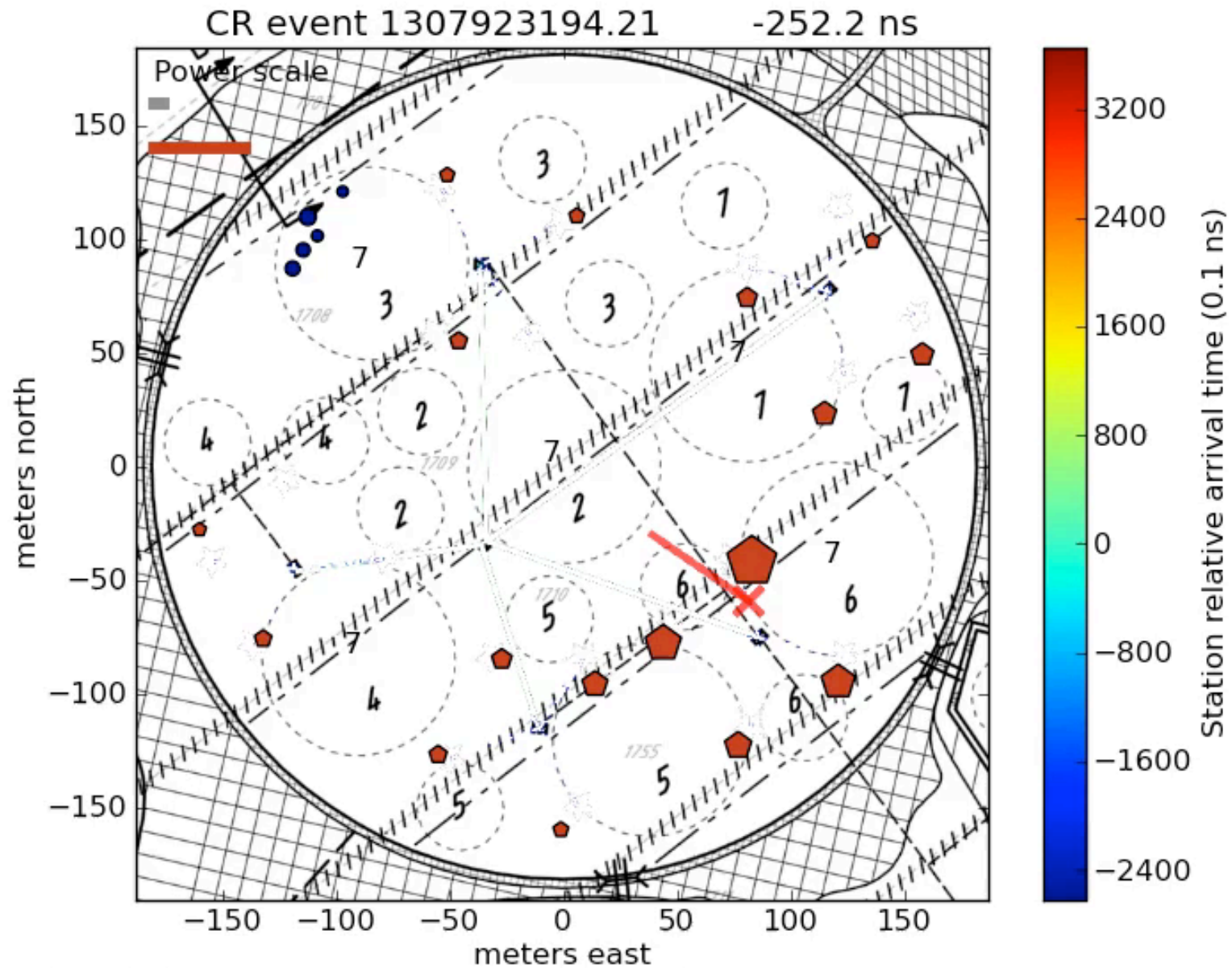


background dominated by
Galactic emission



Lateral Distribution

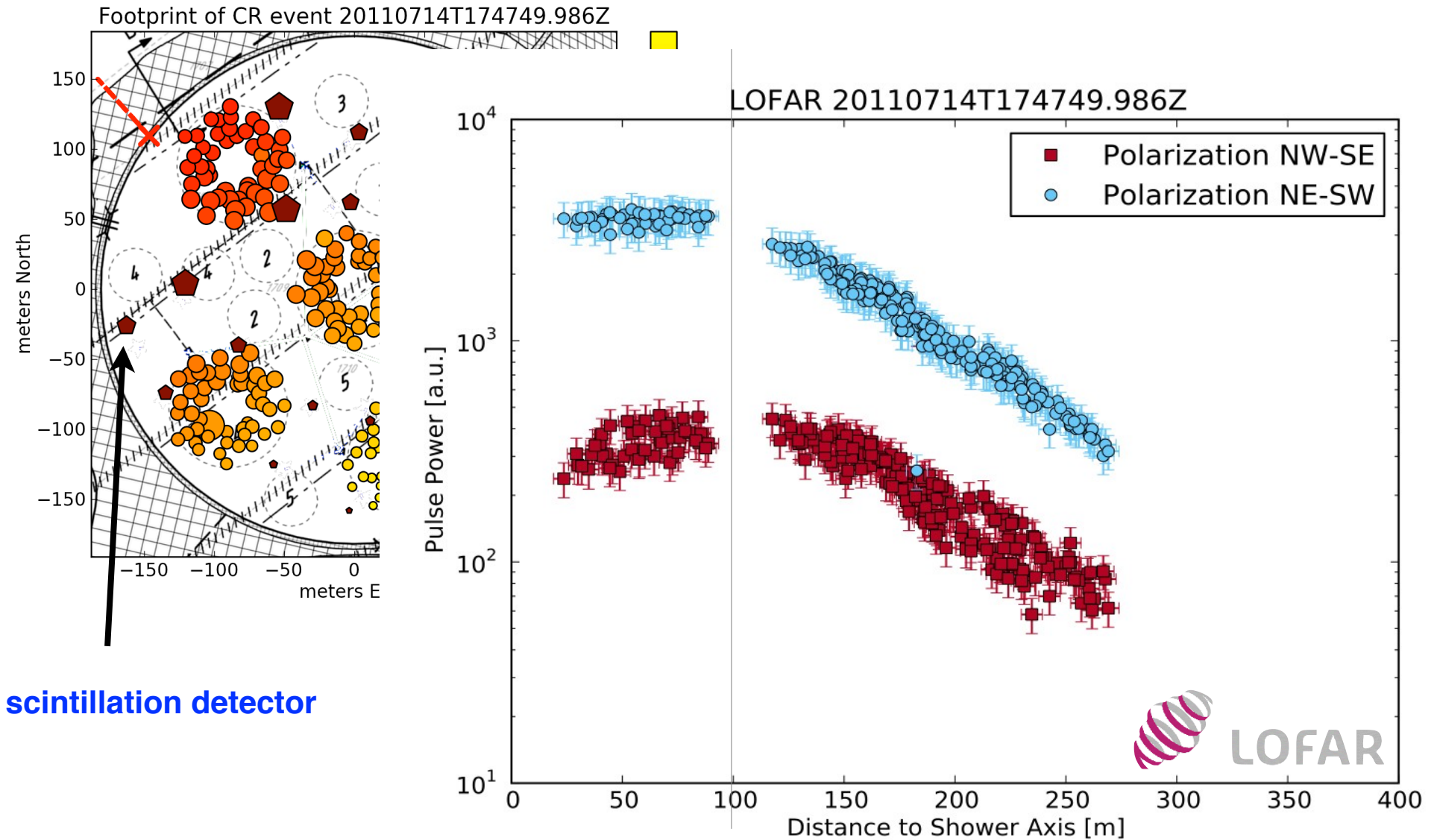
A measured air shower



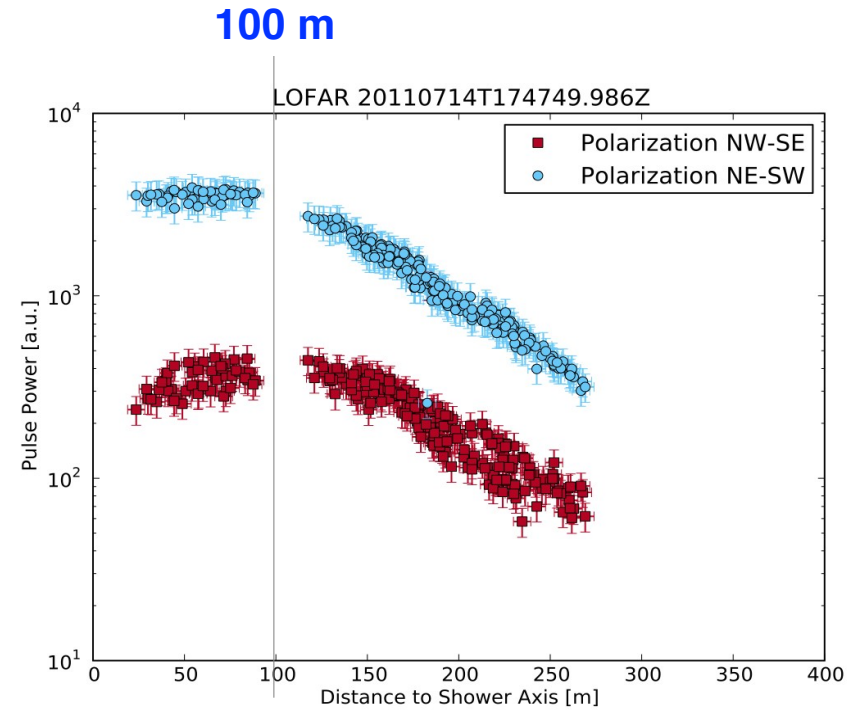
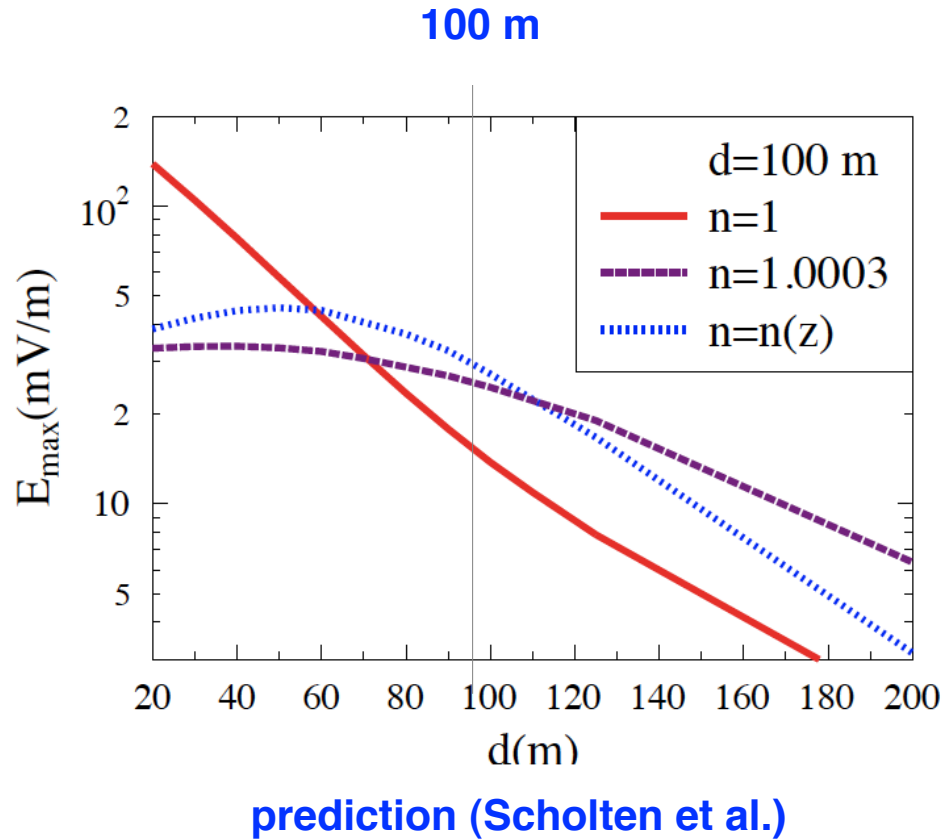
Circles: LOFAR antennas, Pentagons: LORA particle detectors, size denotes signal strength

A measured air shower

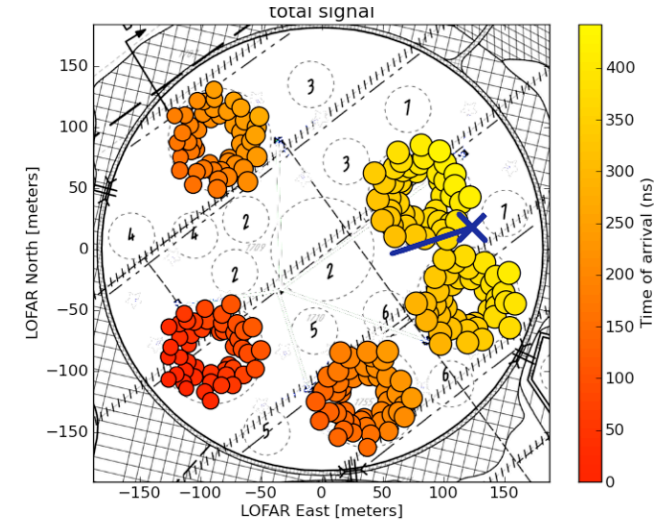
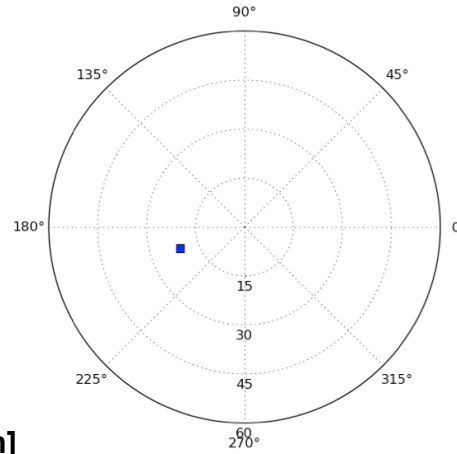
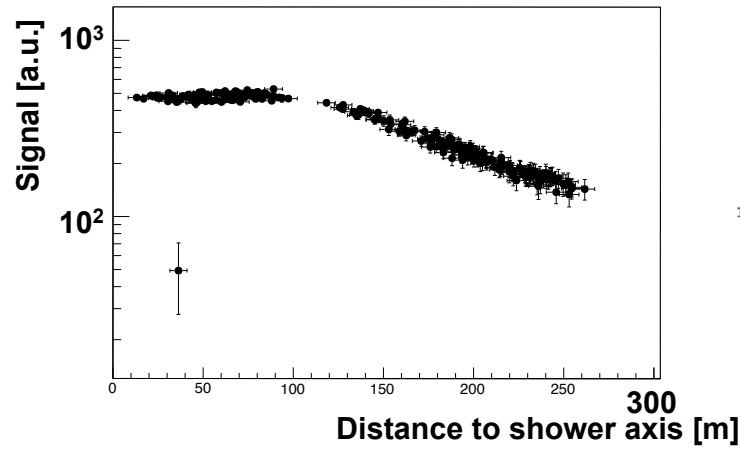
lateral distribution



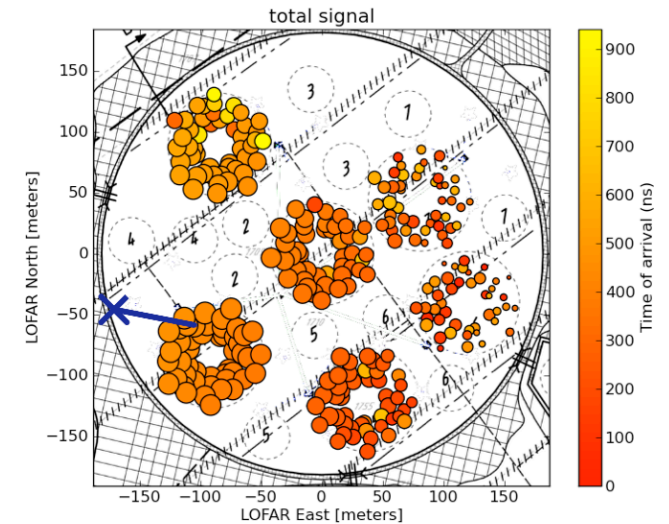
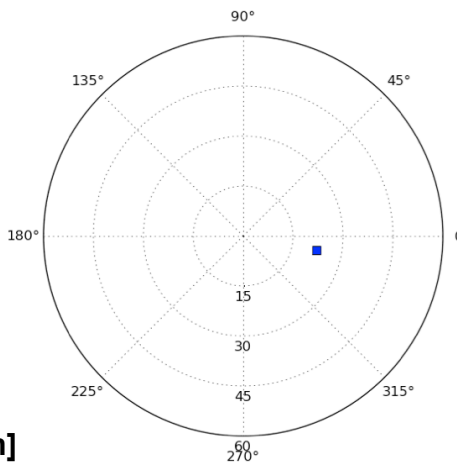
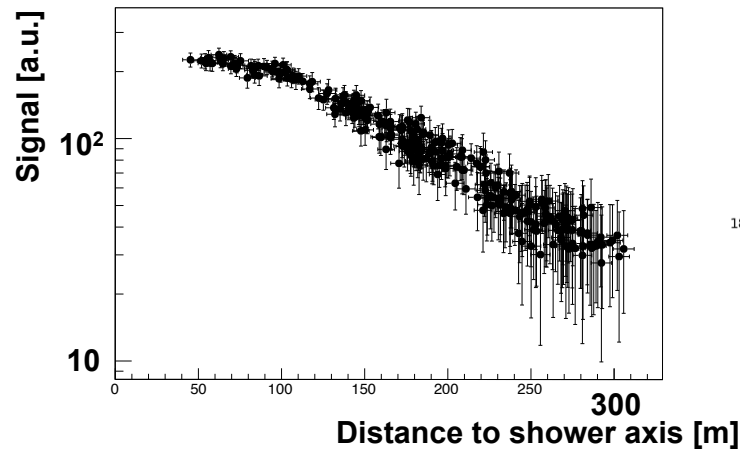
Measured lateral distribution of radio signal



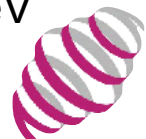
Measured air showers



Energy: 1.2×10^{17} eV



Energy: 3.5×10^{16} eV

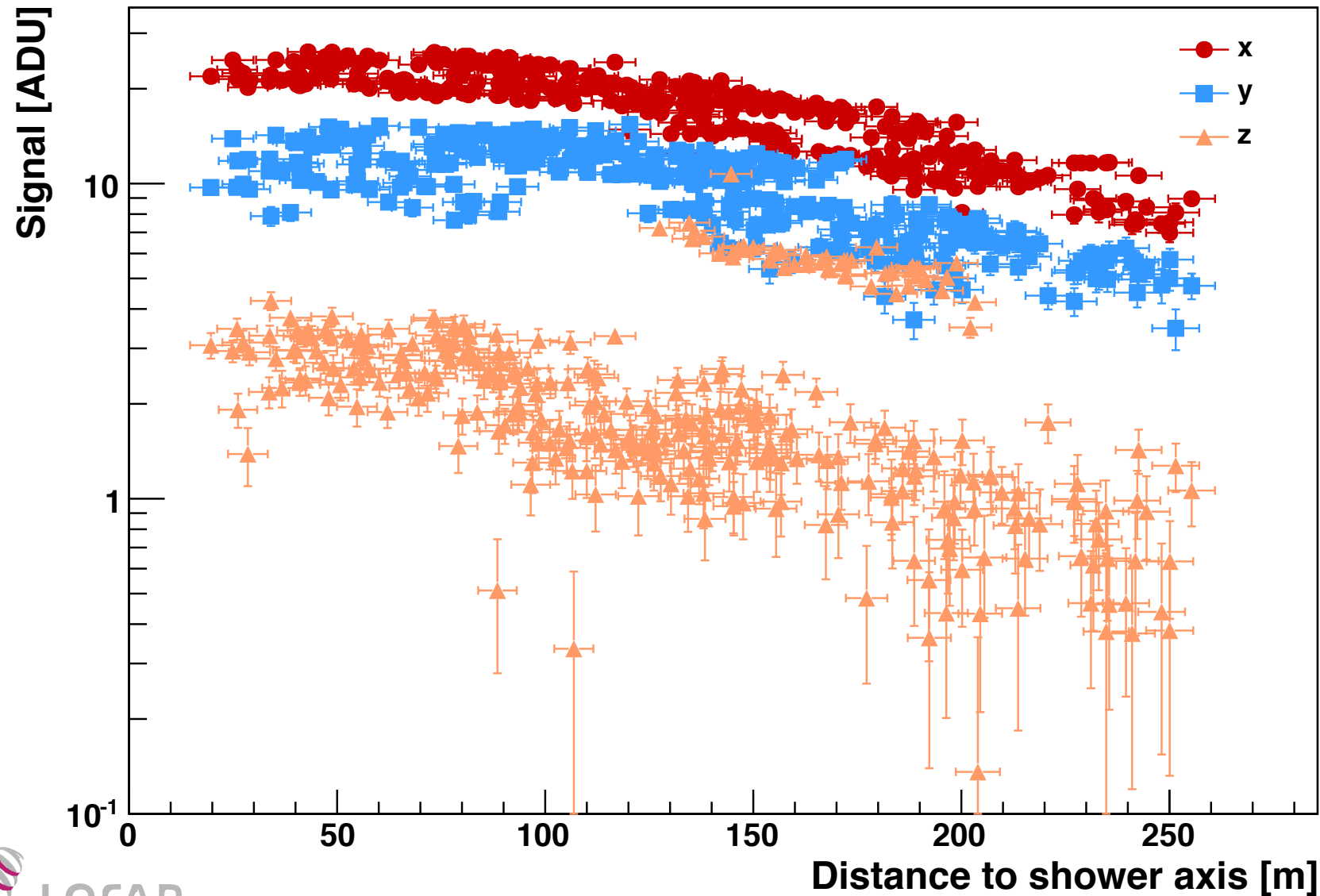


LOFAR

Energy uncertainty from LORA: $\sim 30\%$ per event

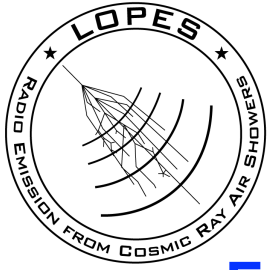
Lateral distribution in 3 polarization components

A measured air shower



Polarization

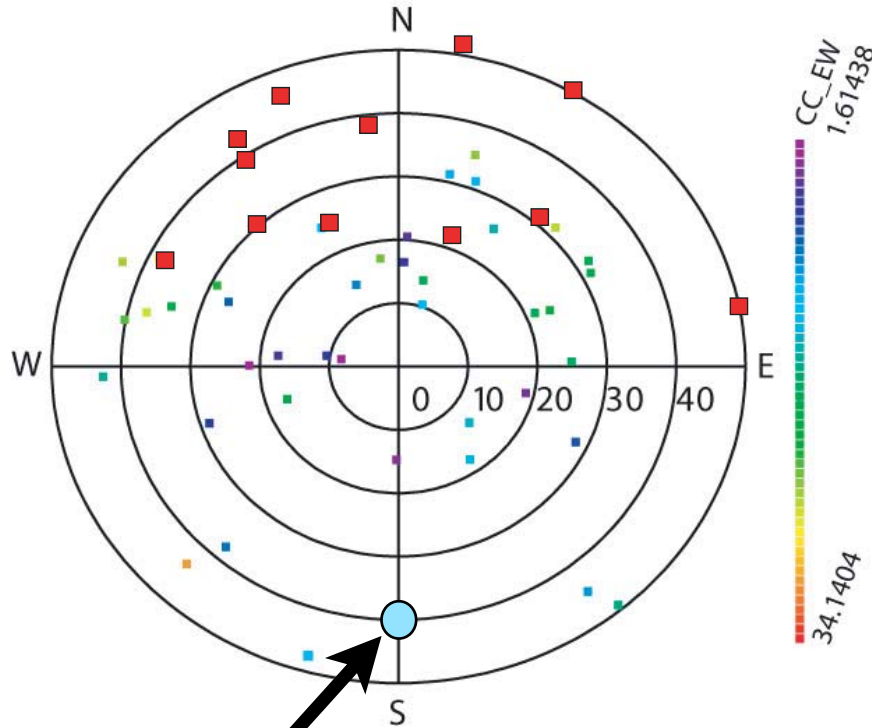




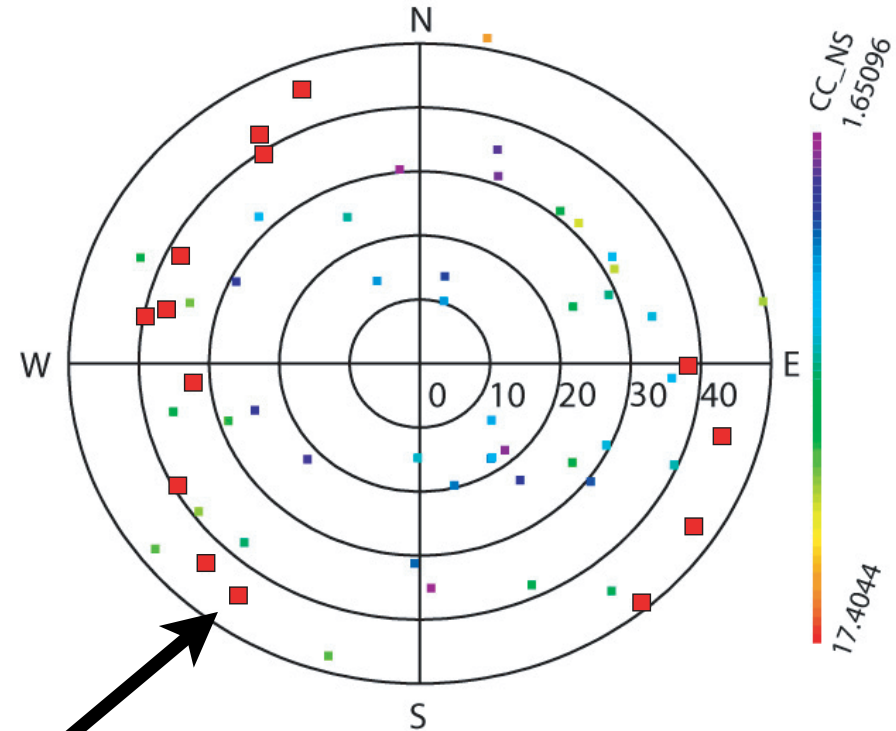
Geosynchrotron component

arrival direction of cosmic rays (sky map)

E-W polarization



N-S polarization



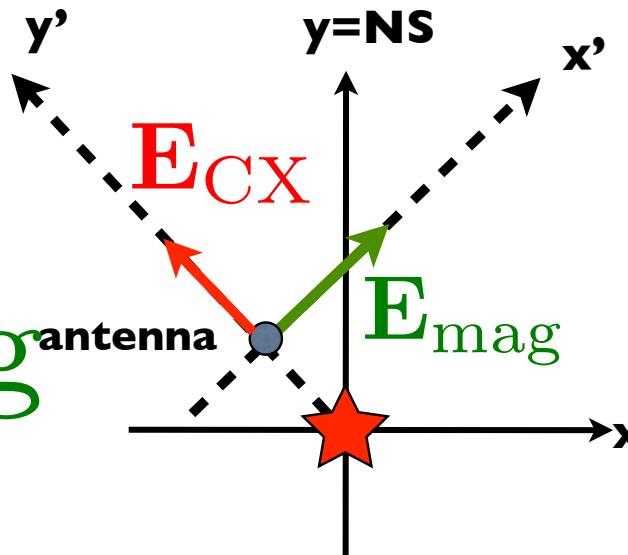
strongest events

magnetic field
inclination: $64^{\circ} 36'$
declination: $1^{\circ} 22'$

$v \times B$ effect
synchrotron radiation dominates signal

P.G. Isar et al., Nucl. Instr. & Meth. A 604(2009) S81

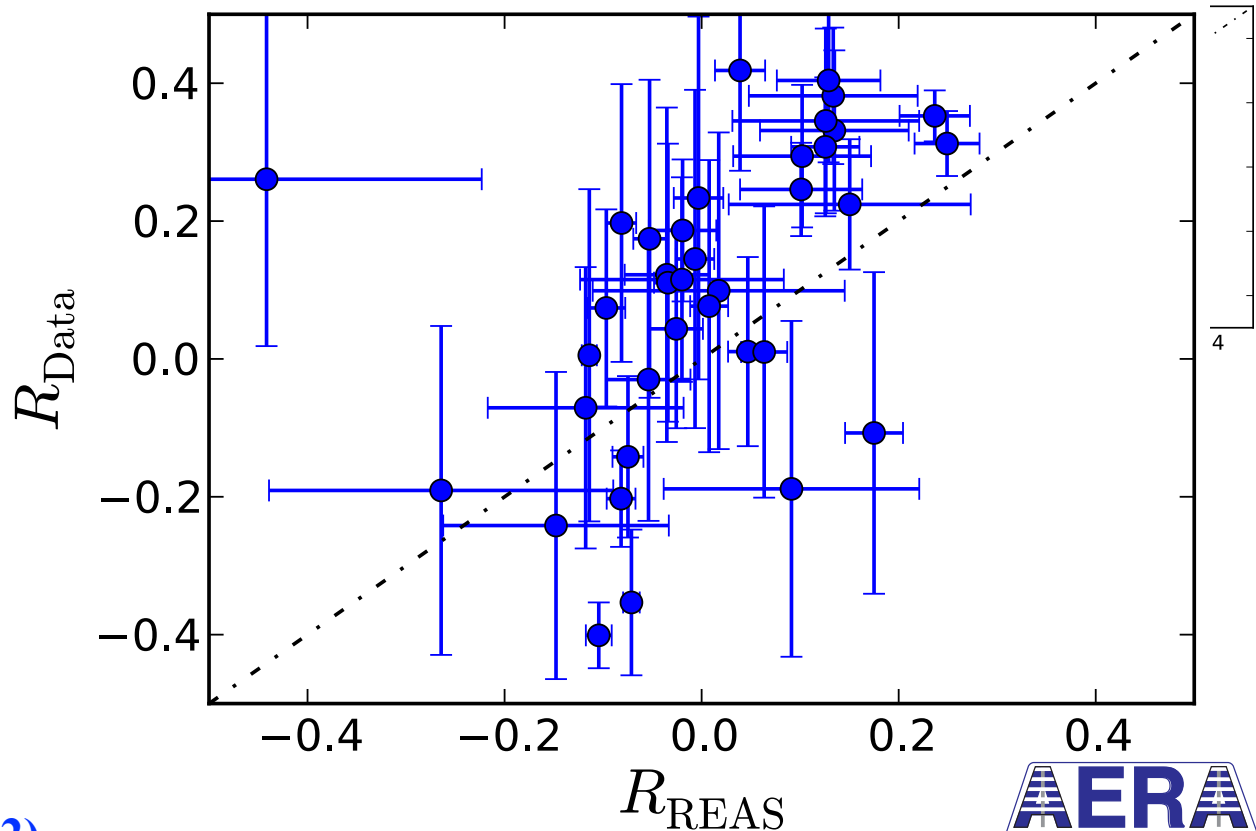
Charge excess component



in (x', y') , define:

$$R = \frac{\sum_{i=1}^N E_{x'}(t_i) E_{y'}(t_i)}{\sum_{i=1}^N E_{x'}^2(t_i) + E_{y'}^2(t_i)}$$

if no charge excess: $R=0$ compare R_{data} and R_{sim}



χ^2/dof values
MGRM
REAS

Direction

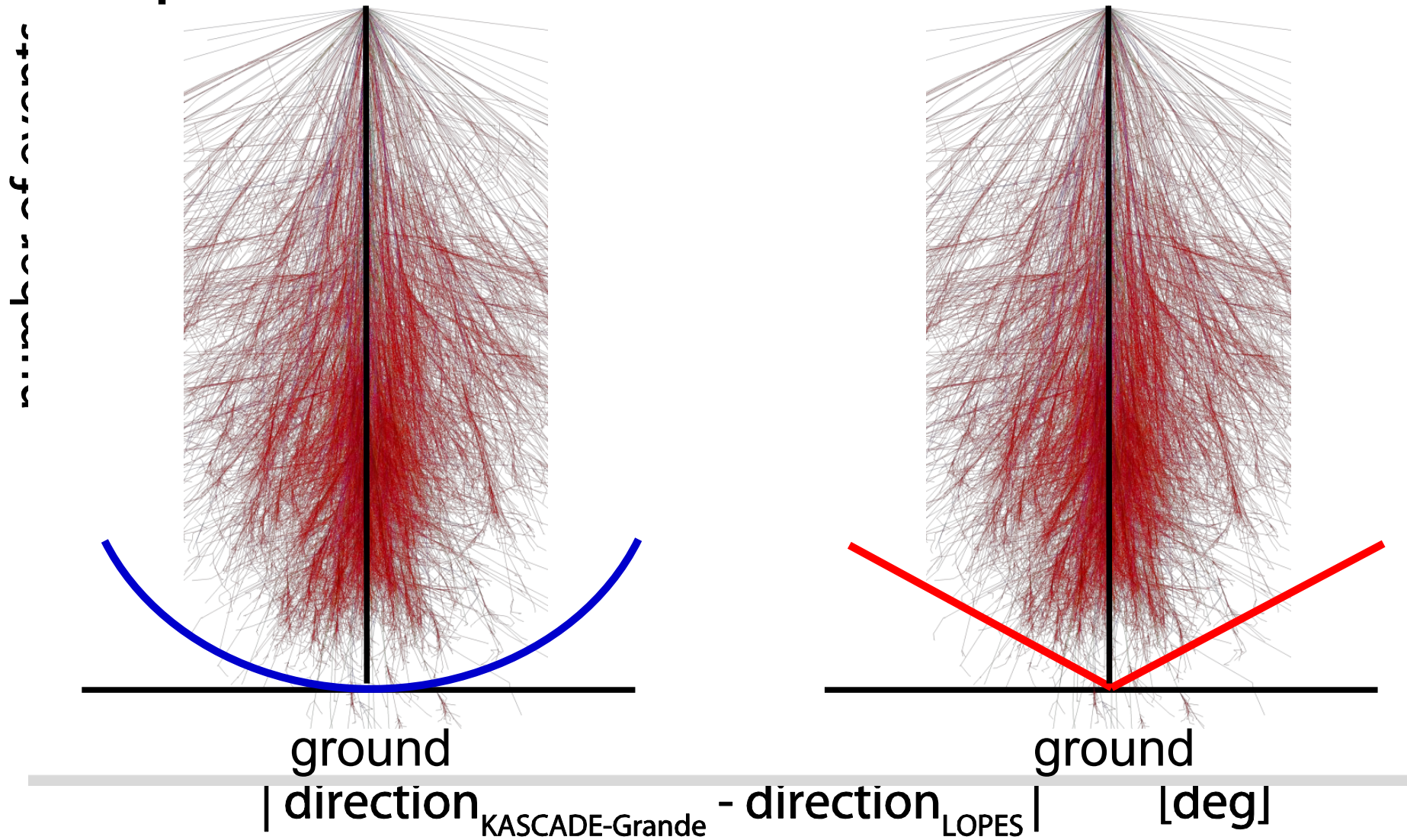




LOPES: direction of shower

spherical wavefront

conical wavefront

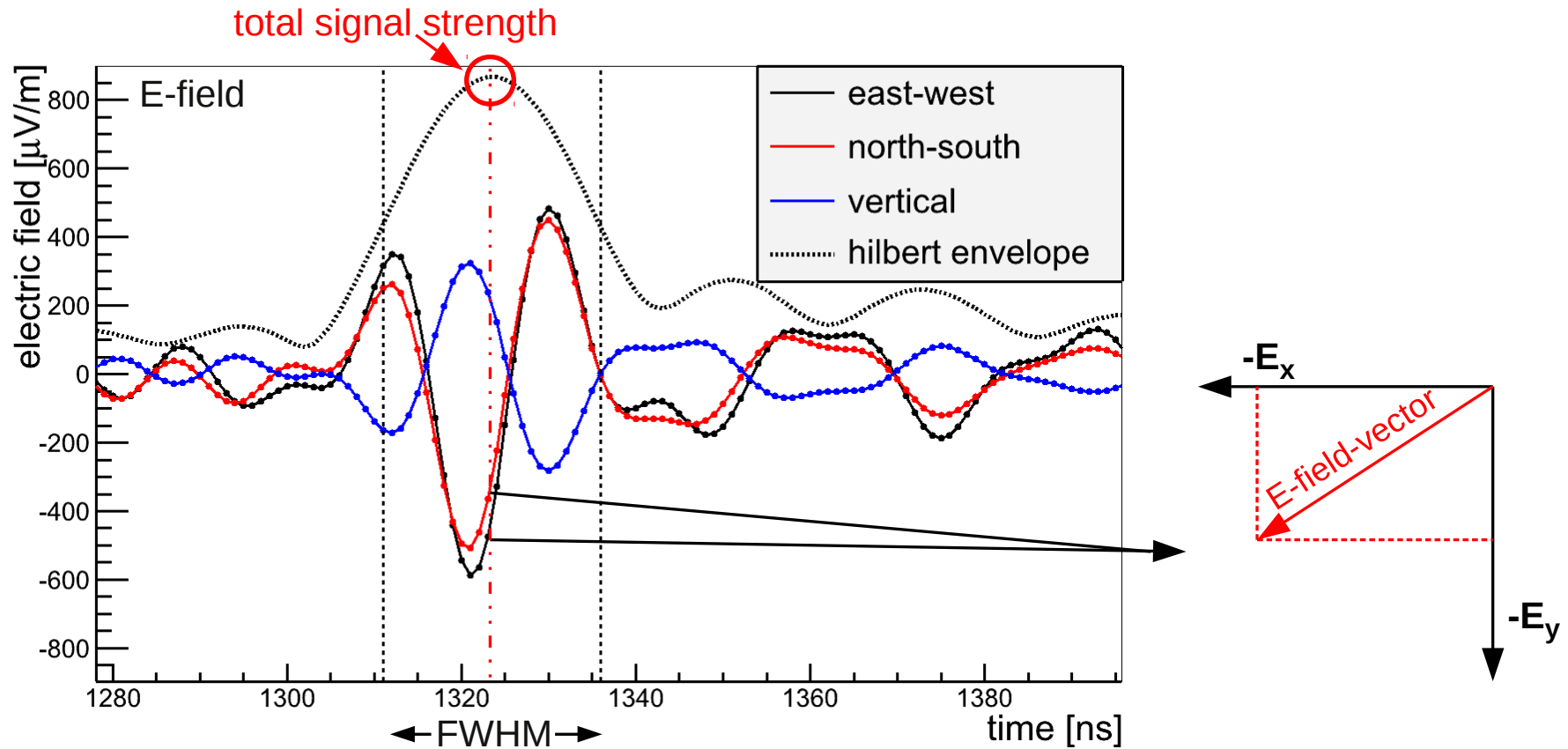


F. Schröder, ARENA (2012)

Energy



AERA: direction of E field vector

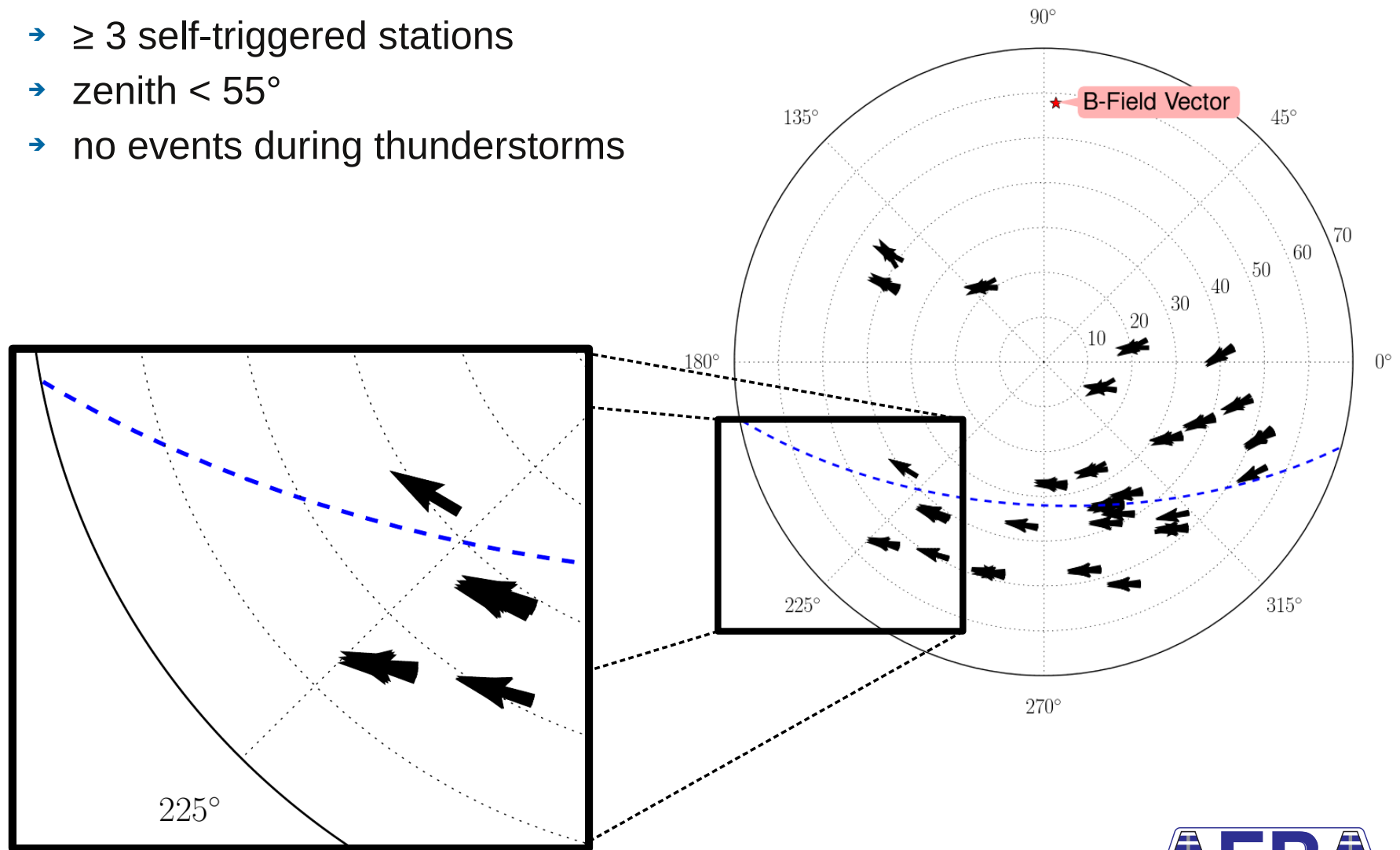


C. Glaser, ARENA (2012)



AERA: direction of E field vector

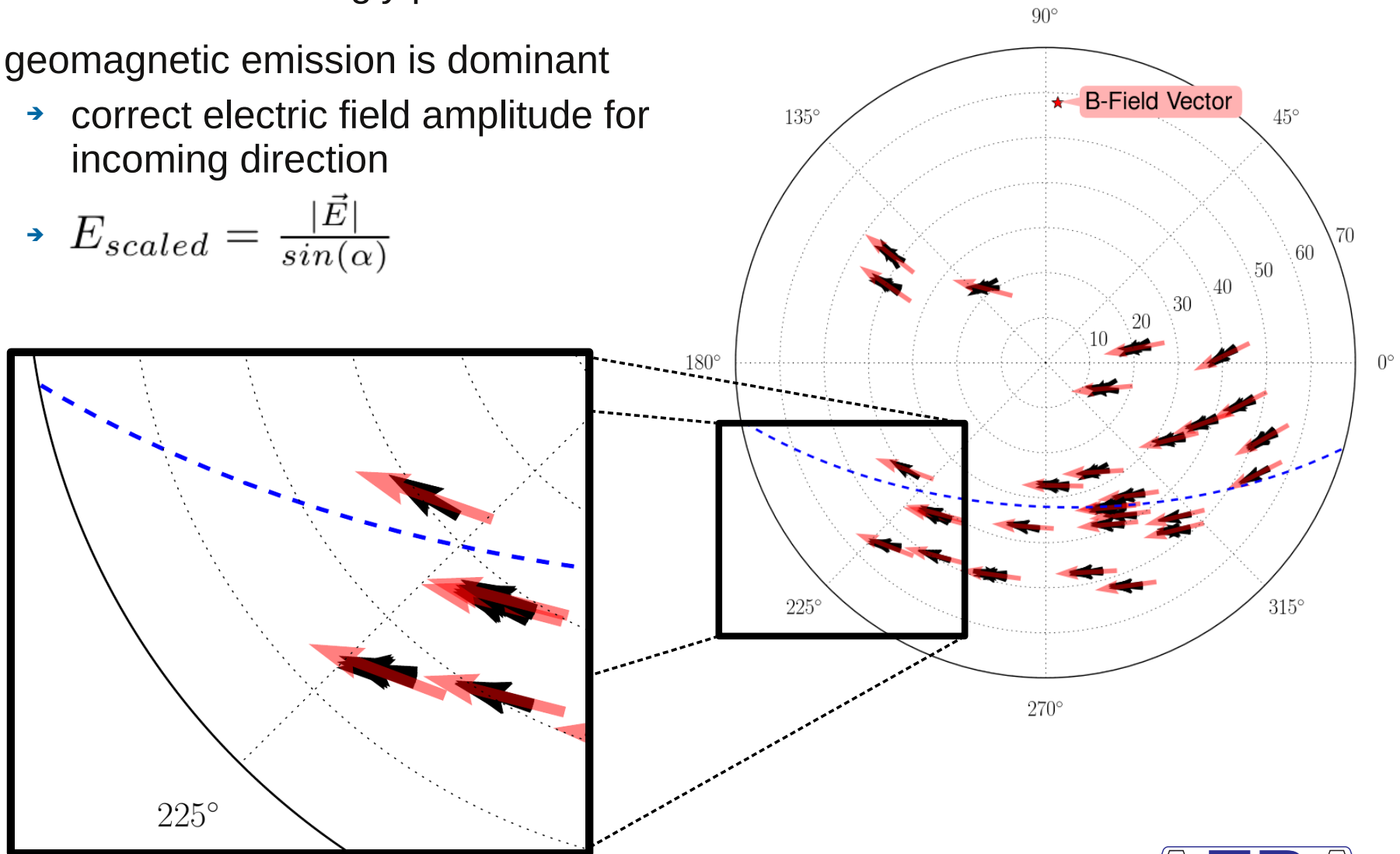
- event selection:
 - ≥ 3 self-triggered stations
 - zenith $< 55^\circ$
 - no events during thunderstorms



C. Glaser, ARENA (2012)

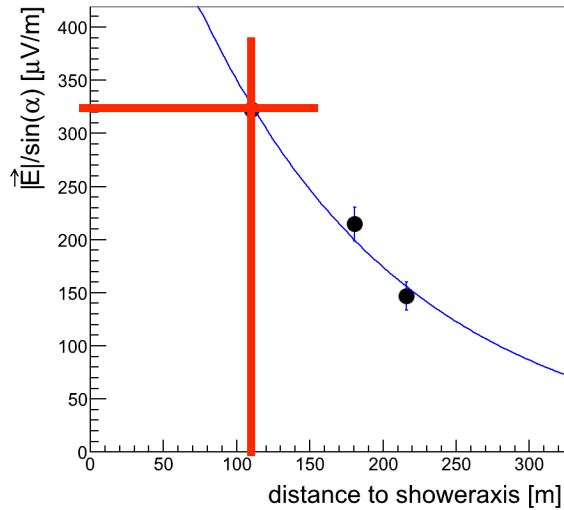
AERA: measured vs. expected values

- electric field is strongly polarised
- geomagnetic emission is dominant
 - correct electric field amplitude for incoming direction
 - $E_{scaled} = \frac{|\vec{E}|}{\sin(\alpha)}$



C. Glaser, ARENA (2012)

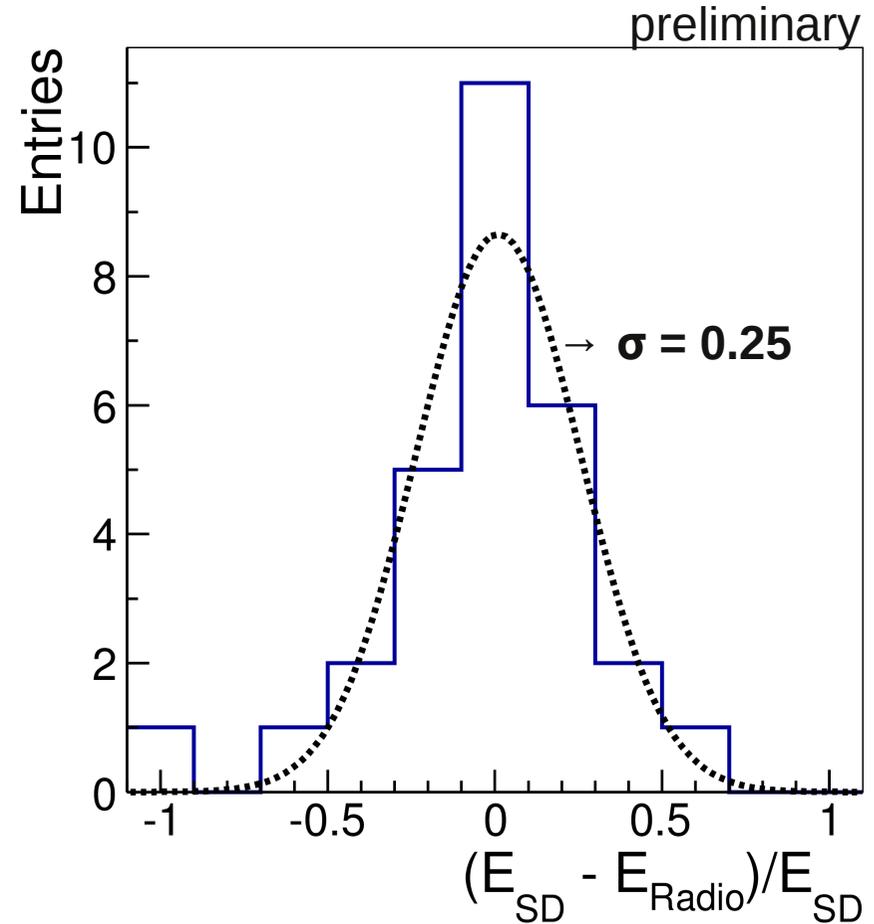
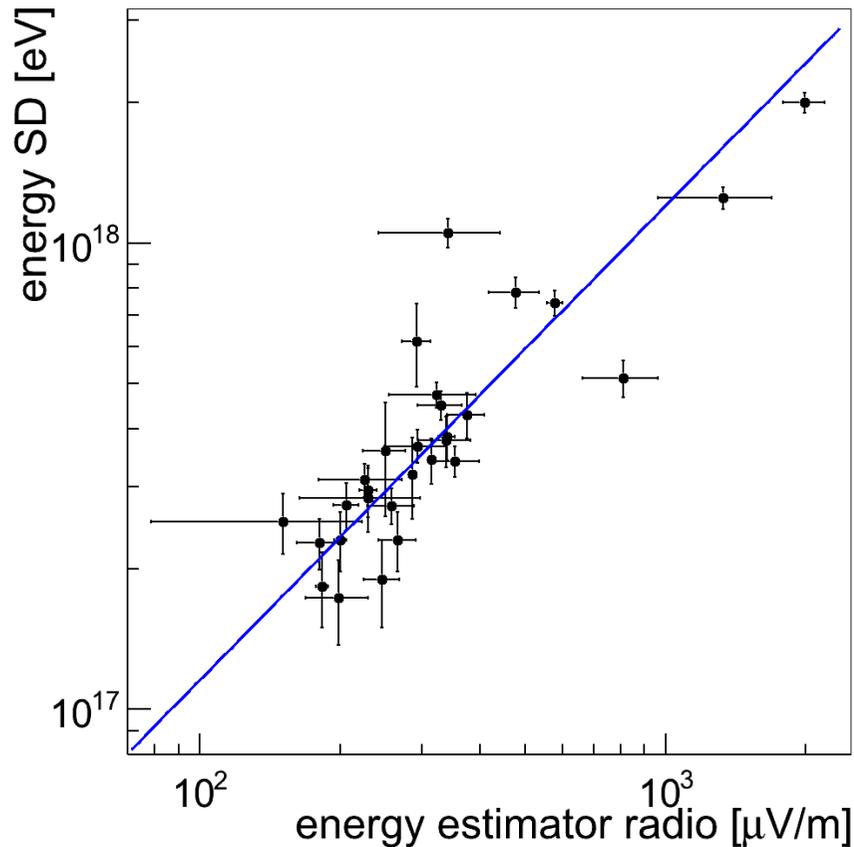
AERA: energy correlation



$$E_{scaled} = \frac{|\vec{E}|}{\sin(\alpha)}$$

$$E_{scaled} = A \cdot \exp(D/R_0)$$

energy resolution 25%
(incl. surface detector resolution)

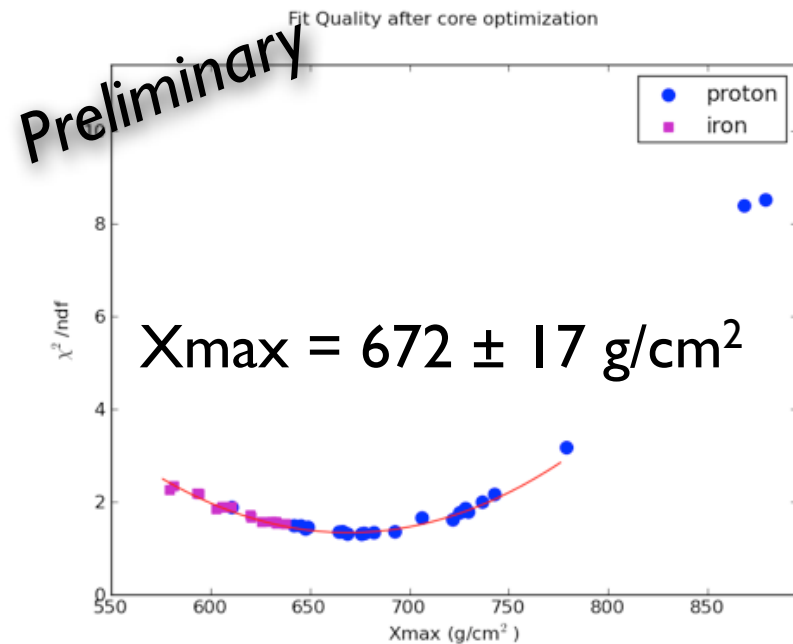
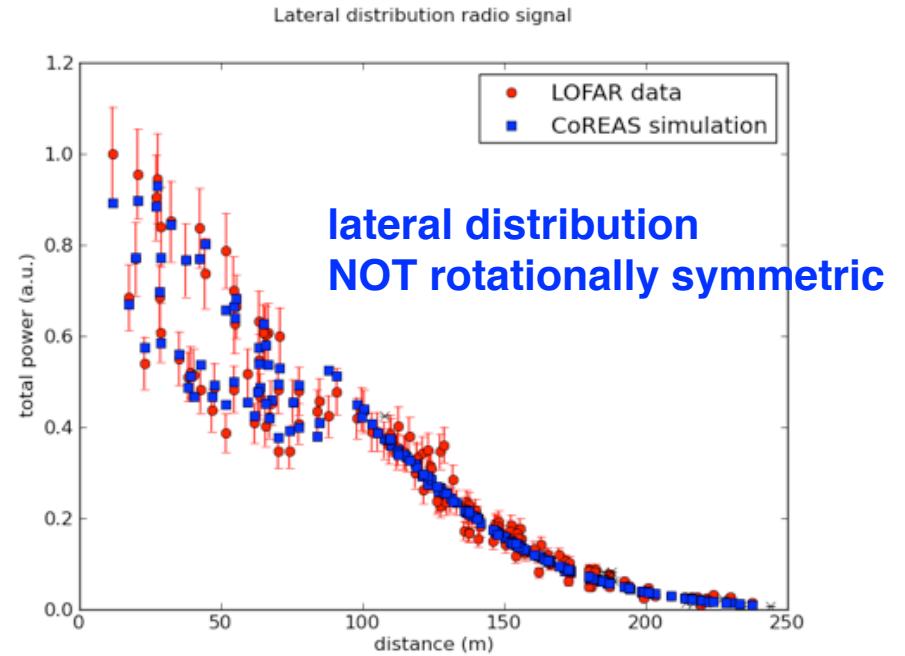
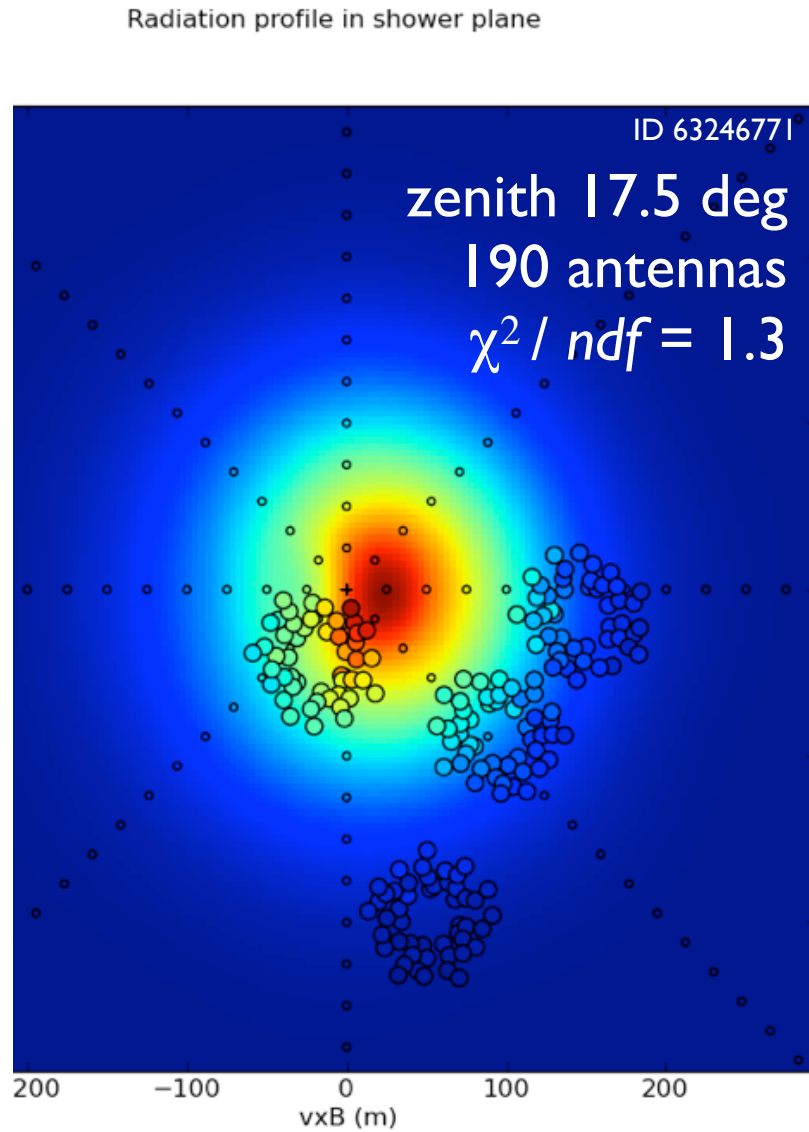


C. Glaser, ARENA (2012)

Mass



First measurement of Xmax with the radio technique



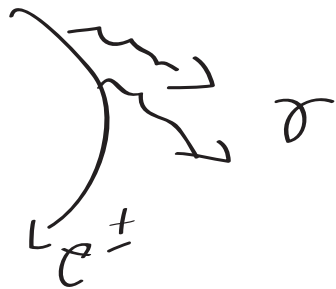
High energy γ rays

In addition to charged particles we obtain information on the high-energy universe from γ -rays

$$\bar{E} \sim 100 \text{ MeV} \rightarrow 50 \text{ TeV}$$

Production & interactions

1) synchrotron radiation of electrons in B fields depending on the energy of electrons

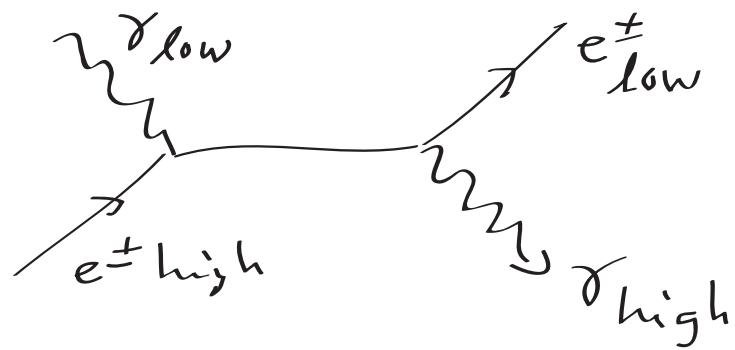


and strength of B field, the

energy of photons ranges from radio (meV) to $\sim 10 \text{ MeV}$

$$\bar{E}_\gamma \propto B^2 \cdot \gamma_e^2 \quad \text{radiation is polarized}$$

2) Inverse Compton Scattering



energy of electrons
is transferred to
photons

"heating of photons
through electrons"

$$\bar{E}_\gamma \propto U_{\text{rad}} \cdot \delta_e^2$$

↑
temperature (kinetic energy) of photons

3) Hadronic interactions



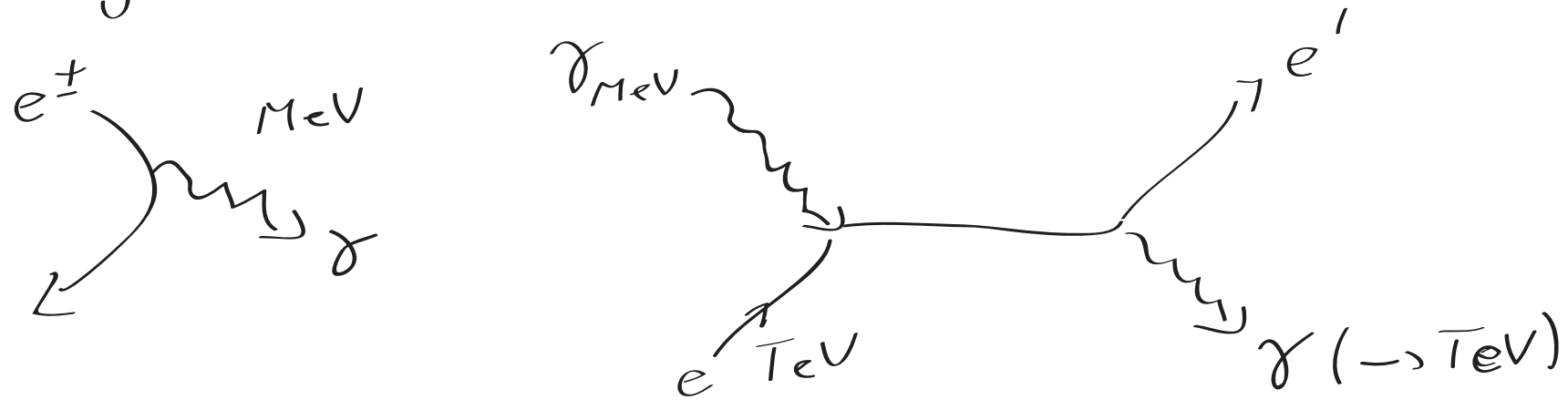
requires presence of hadronic particles

4) Bremsstrahlung

$e + \text{target} \rightarrow \text{Bremsstrahlung}$

$$E_\gamma \sim \frac{E_e}{2} \quad (\text{power law})$$

important combination of 1 & 2
synchrotron self Compton (SSC)



the photons for inverse Compton scattering
are produced in situ

